TECHNICAL NOTE R-119

A REVIEW OF GOVERNING PROCESSES

AND LIQUID CAVITATION PHENOMENA

FOR FLOW IN CURVED DUCTS

by Gerald R. Guinn

October 1964

RESEARCH LABORATORIES

BROWN ENGINEERING COMPANY, INC.

HUNTSVILLE, ALABAMA

TECHNICAL NOTE R-119

A REVIEW OF GOVERNING PROCESSES
AND LIQUID CAVITATION PHENOMENA
FOR FLOW IN CURVED DUCTS

October 1964

Prepared For

APPLIED MECHANICAL RESEARCH BRANCH
PROPULSION DIVISION
P&VE LABORATORY
GEORGE C. MARSHALL SPACE FLIGHT CENTER

By

RESEARCH LABORATORIES
BROWN ENGINEERING COMPANY, INC.

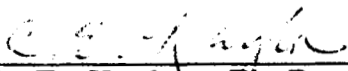Contract NAS8-11166

Prepared By

G. R. Guinn

ABSTRACT

A review of literature pertaining to flow in curved pipes was conducted. The primary emphasis was directed towards presenting a description of the curved flow processes, especially those that influence cavitation and downstream flow distortion. The flow field in an elbow has been described as being divisible into three regions which are (1) the inviscid central core, (2) the viscous shedding layer and (3) the region of eddy flow. For turbulent flow, the regions are quite distinct and the central core corresponds approximately to potential flow. The flow distortions arising in the bend are oscillatory in nature and are observed to persist a great distance downstream with a strong dependence upon the entrance conditions. Analytical treatments of curved pipe flow have been primarily confined to fully developed coiled pipe flow. It was concluded that there is inadequate experimental and analytical information available for solutions to problems arising in ducting the propellants of liquid rocket engines.

Approved

C. E. Kaylor, Ph. D.
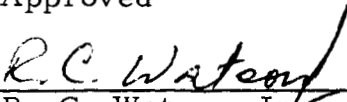Director, Mechanics and
   Propulsion Laboratories

Approved

R. C. Watson, Jr.
Director of Research

TABLE OF CONTENTS

LIST OF FIGURES

LIST OF FIGURES (Continued)

LIST OF SYMBOLS

A	Cross sectional flow area
a	Pipe radius
C_d	Flow rate discharge coefficient defined in Equation 19
C_p	Pressure coefficient defined in Equation 1
$C_{p_{min}}$	Pressure coefficient based on minimum pressure, Equation 4
D	Dean's number defined in Equation 9
g	Gravitational acceleration constant
h_{1_i}	Cavitation inception static reference head
K	Constant defined by Equation 15
$\dot{m}$	Weight flow rate
P	Total pressure
p	Absolute static pressure
p_1	Absolute static pressure at some reference station
p_i	Static pressure at the inside wall of a pipe bend
p_m	Static pressure at the position where the velocity is equal to the mean velocity
p_o	Static pressure on the outside wall of a pipe bend
p_v	Vapor pressure of the liquid
p_{min}	Minimum static pressure in a flow field
R	Elbow centerline radius of curvature
Re	Reynolds number $\left(= \dfrac{2 \rho W a}{\mu} \right)$
r'	Streamline radius of curvature
W	Mass average axial velocity

LIST OF SYMBOLS (Continued)

w'   Velocity component tangential to r'

ζ Curved pipe resistance coefficient ratio

θ Pipe bend deflection angle

μ Dynamic viscosity

ρ Liquid density

σ Thoma-Moody cavitation number

σ_i Inception cavitation number

INTRODUCTION

Elbows and pipe bends are potential sources of cavitation and flow distortion in the propellant lines of liquid rocket engines. This is particularly true for the sharp turns and high flow rates required to meet the stringent weight and space limitations of such applications. Unfortunately there has been no adequate study of flow distortion and no systematic investigation of cavitation in such configurations. The purpose of this effort is to review some previous research, both experimental and analytical, in an attempt to obtain an insight into the factors influencing liquid cavitation and flow distortion arising from the flow phenomena in elbows and pipe bends which may be located in the propellant system of liquid rocket engines.

The primary influence of a duct elbow in a flow system is to generate greater total head losses than would normally occur in a straight duct of equal length. However, if the elbow is located in a propellant line near the suction side of a pump for a liquid propellant rocket engine, the fluid will approach the inlet in a disoriented and nonuniform manner, especially if separation occurs within the elbow or the velocity profile at the elbow entrance possesses a certain asymmetry. The most efficient pump design requires that the approaching flow be as uniform as possible so that the impeller blades can be designed for the proper relative velocities without introducing unnecessary compromises. Space or weight limitations may preclude the use of guide vanes or a length of straight pipe run before the pump entrance; hence, it is desirable that the elbow be designed in such a manner so as to disturb the flow as little as possible.

Cavitation in the proximate elbow may introduce additional reductions in the pump efficiency. Because of hysteresis associated with the formation and disappearance of cavitation bubbles, the vaporous pockets formed in a cavitating elbow may persist in a supercooled state for some distance downstream before collapse. If these bubbles enter

1

the pump, they will form "weak" spots in the liquid and thus provide the nuclei for possible premature inception of cavitation within the pump itself and with a drastic reduction in pump efficiency as a result.

To avoid cavitation within the pump and the upstream ducting system containing pipe bends, it is necessary to bring the liquid to the inlet section of the pump under a sufficiently high static pressure, obtained either by auxiliary pumps or by pressurizing the propellant tanks. Since either technique introduces an additional weight penalty to the propulsion system, it is desirable to design the components of the pump feed system, e.g., elbows, so that a minimum weight system is achieved but in such a manner that cavitation within the pump itself is not induced.

The prediction of cavitation inception characteristics of a particular elbow design requires, at the very minimum, a knowledge of the vapor pressure of the liquid and the pressure coefficient of the elbow which may be defined as follows:

$$C_p = \frac{p_1 - p}{\dfrac{\rho W^2}{2g}} \tag{1}$$

where p_1 is the static pressure taken immediately upstream of the bend but sufficiently far from the bend so that the pressure is uniform across the pipe and p is the local static pressure at any desired point within the flow field. Also W is the average velocity at the same reference location as p_1 and is defined by

$$W = \frac{\dot{m}}{\rho A} \tag{2}$$

where $\dot{m}$ is the weight flow rate through the pipe and A is the cross sectional flow area at the reference location.

Unfortunately, due to the complex three-dimensional nature of the flow, there exists, at the moment, no satisfactory means of predicting

the pressures within a duct elbow with a circular cross section or of predicting the flow patterns in the downstream pipe. However, various aspects of this type of flow have been experimentally and analytically investigated to some degree, cavitation being an exception. As an aid to future studies, it is the purpose of this report to review some of these investigations in an effort to provide an understanding of the fundamental nature of flow in a pipe elbow. For brevity, only those references will be reviewed that represent the state of knowledge of curved ducts and judged to contribute most to the understanding of the present problem. A bibliography of related references will be provided for those interested in pursuing the subject in greater detail.

The author wishes to acknowledge the assistance and cooperation of his coworkers, Mr. E. H. Ingram and Mr. Carl T. K. Young, in the preparation of this report and in the clarification of the problems involved by their stimulating discussions.

TECHNICAL DISCUSSION

Cavitation

Cavitation has long been a source of problems to hydraulic and marine engineers. It can create undesirable noise and vibration and reduce the efficiency of hydraulic structures. Prolonged operation under cavitation conditions can attack the surfaces and result in pitting or erosion and quite possibly destruction of the equipment insofar as satisfactory operation is concerned.

Cavitation can be particularly troublesome in the pumps and the lines that transport the propellants for liquid propellant rocket engines. It is a primary consideration in the design of liquid pumps and imposes a number of restrictions on their operating limits and efficiency. For this reason, cavitation in pumps has been studied quite extensively. The cavitation of a liquid in curved ducts has received some attention from early investigators primarily as post facto studies of the damage to dam conduits. Insofar as could be determined, little attention has been devoted to cavitation within curved ducts in the more modern applications to liquid rocket propellant feed systems.

Cavitation is the formation and subsequent collapse of holes or voids in a liquid when the local static pressure at some point decreases to approximately the vapor pressure and then increases as the slug of fluid progresses downstream. The cavities may appear as a result of dissolved gases being released from the solution or of local boiling of the liquid itself. The pressure variations may occur from a vortex system or from velocity changes as the fluid conforms to the solid boundaries of a duct or an immersed object.

There are a number of factors which influence the onset of cavitation. The dissolved gas content may strongly affect the pressures at which cavitation begins to appear since the gas may come out of solution

4

when the pressure is still far above the vapor pressure of the liquid. The gas content influences the compressibility of the surrounding liquid and hence the propagation characteristic of the cavitation induced pressure variations, especially those arising during the rapid collapse of the bubbles on reaching a region of pressure greater than the vapor pressure.

The formation of a cavity or bubble is also dependent upon the surface tension of the liquid. Here again the gas content as well as the liquid temperature and the presence of any dissolved impurities exercises an influence even if in minute concentrations. External influences such as noise level, heat transfer, turbulence level, surface roughness, and fluid intermolecular properties such as viscosity, thermal conductivity and the mass diffusion coefficient may also play an important role in the cavitation process. Because of the expense associated with testing prototype hardware, scaling laws governing the various factors influencing cavitation are of considerable importance in cavitation experiments. Because of the large number of variables involved, the efforts to find similarity or scaling laws encompassing all of the aforementioned effects has, unfortunately, not been completely successful.

The problem is not completely hopeless, however, because of the relatively minor role most of these effects play and the dominant role of a few. The following discussion illustrates the scaling of the vapor pressure which is by far the most important liquid property to consider for cavitation studies.

The pressure coefficient for noncavitation flow associated with a structure of specified geometry is defined to be

$$C_p = \frac{p_1 - p}{\frac{\rho W^2}{2g}} \tag{3}$$

where p_1 is some reference static pressure in the flow field, p is the static pressure at any location on the body or in the flow field, ρ is the density of the fluid and W is the mean fluid velocity.

5

The "minimum pressure coefficient" occurs at a point on the bounding surface or in the enveloping flow where the static pressure is a minimum (the pressure coefficient is a maximum) and is defined as

$$C_{P_{min}} = \frac{p_1 - p_{min}}{\dfrac{\rho W^2}{2g}} \qquad . \qquad (4)$$

The most important effect related to the scaling of cavitation is the vapor pressure of the liquid at the prevailing liquid temperature. The scaling parameter incorporating the vapor pressure is called the "Thoma-Moody cavitation number", which is defined as

$$\sigma = \frac{p_1 - p_v}{\dfrac{\rho W^2}{2g}} \qquad (5)$$

where p_v is the vapor pressure of the liquid.

There are two important stages associated with the cavitation process. The most advanced occurs when the vapor pressure is high with respect to the local static pressure and profuse cavitation is present. This is called the "cavity flow" regime wherein an extensive vapor pocket is formed and the cavitation process and the flow field are coupled so that cavitation influences the pressure distribution over the body, depending upon the size of the pocket. The second regime occurs when the vapor pressure is approximately equal to the local static pressure so that only a limited number of cavitation bubbles appear. This is called "incipient cavitation" regime where the voids comprise a negligible portion of the fluid volume so that the noncavitation static pressure distribution is not altered by the cavitation process. If flow conditions are such that cavitation is just apparent (incipient cavitation), then under ideal conditions where cavitation is due only to the vaporous formation of voids, the local static pressure is equal to the vapor pressure and

$$\sigma_i = C_{P_{min}} \qquad (6)$$

6

where σ_i is defined as the inception cavitation number. Tests with degassed liquids have indicated that, because of the aforementioned scale effects, there is a time lag in the rate of formation of cavities and hence the minimum static pressure may often become less than the vapor pressure before the inception of cavitation. Therefore, the relation for vaporous cavitation is generally

$$\sigma_i \leq C_{P_{min}} \tag{7a}$$

i.e.,

$$P_{min} \leq P_v \tag{7b}$$

for the specified conditions.

If there is a significant amount of gas dissolved in the liquid, then cavitation will appear prematurely because of the effervescence of the gases out of solution, therefore for this less common situation

$$\sigma_i > C_{P_{min}} \tag{8}$$

i.e., cavitation will appear before the local static pressure has depressed to the vapor pressure of the liquid.

The preceding discussions form the basis for a hydrodynamic determination of the inception of cavitation for a particular flow condition. That is, if one can predict the static pressure variation for a desired configuration under noncavitation conditions, then, since Equation 7 is valid under most circumstances, this will enable one to at least estimate whether or not cavitation will occur at those conditions. It does not enable one to determine for what conditions cavitation will occur unless additional information is available from experimental sources.

Flow Characteristics in a Pipe Bend

Fluid particles passing through a pipe bend of circular cross section follow a very complex, three-dimensional path. The conditions of the fluid

7

at the entrance to a bend are established by the upstream ducting system, and as a result the velocity is generally nonuniform because of viscous resistance of the walls or obstructions that disarrange the flow. Due to the variations in the entering fluid velocity, a nonuniform centrifugal force acts on the fluid as the particles traverse individual curved trajectories through the pipe bend. This unbalance of centrifugal force leads to the formation of a secondary flow system which is oscillatory in nature and is directed outwards at the center of the pipe and inwards near the wall; the fluid elements moving along the pipe in two sets of spirals which are separated by the central plane of curvature which contains the centerlines of the two elbow tangents (Figure 1). The influence of the elbow on the flow extends for many diameters into the downstream tangent until the secondary flow system is damped from viscous forces and fully developed pipe flow is established. In effect, the complex flow patterns arise from the nonuniform fluid velocity as it enters the bend and the resultant unbalance of centrifugal forces acting upon the flow in the bend. Thus, any conditions affecting the entering velocity profile would also influence the flow in the bend and downstream tangent such as (1) lack of fully developed pipe flow, (2) laminar or turbulent flow, and (3) distortions arising from other upstream bends, valves, orifices, etc.

The duct downstream of the bend may also affect the flow in the bend itself. Since several diameters may be required for the pressure to become uniform across the downstream duct, curtailment of the downstream bend tangent will place a constraint on the distance away from the bend to which pressure variations may extend, thus increasing the magnitudes of the relative pressure differences within the bend itself.

A pressure gradient across the bend to balance the centrifugal forces acting upon the fluid is also generated by the curvilinear flow. The pressure on the outside of the bend becomes larger than the initial static pressure, attaining some maximum value part way through the bend, and the pressure on the inside, nearer the bend origin becomes
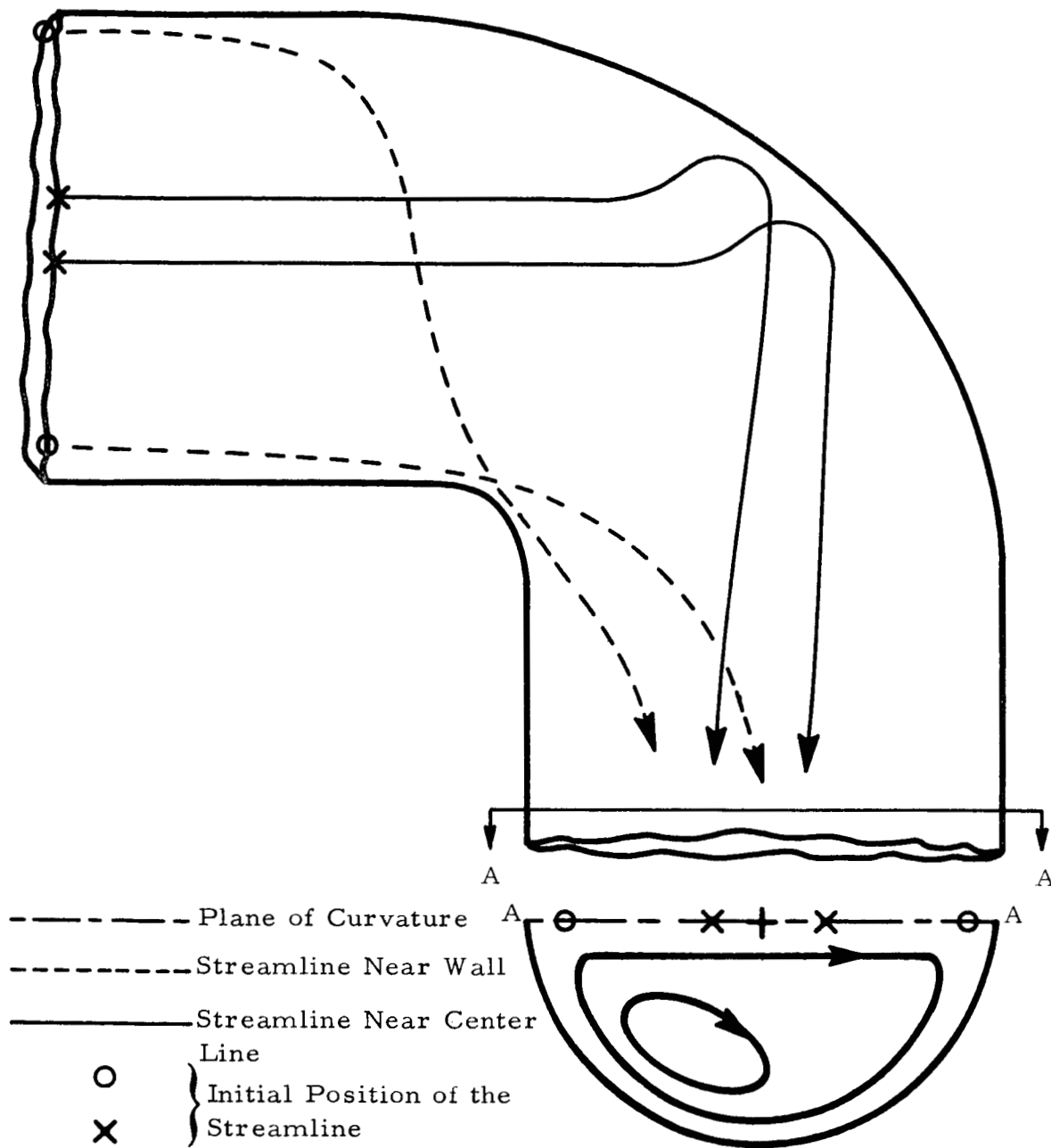
Figure 1. Schematic Representation of the Secondary Flow System in an Elbow of Circular Cross Section

The legend within the figure reads:

— — — Plane of Curvature
- - - - - Streamline Near Wall
——————Streamline Near Center Line
○ ⎫ Initial Position of the
× ⎭ Streamline

smaller than the initial value until some minimum value is reached. Thus as the flow undergoes the transition from rectilinear to curvilinear motion, a positive pressure gradient in the direction of flow is initially imposed on the outer wall of the elbow and then a negative gradient is generated as the static pressure readjusts to a uniform value when the flow leaves the bend. Conversely, on the inner wall, a negative axial pressure gradient is initially present as the pressure decreases to some minimum value at approximately midway through the bend and then a positive gradient is formed as the pressure increases back to a uniform value across the duct downstream of the turn (Figure 2).

When the turning radius is sharp and the flow rates high, the centrifugal forces acting on the flow are large and hence the positive axial pressure gradients may be of sufficient magnitude and extent so that the slow moving fluid particles near the wall lack sufficient momentum to traverse the region of increasing pressure. If this is the case, the particles will reverse their original direction of motion and create a local region of eddies and vortexing near the duct boundaries. That is, the main flow fails to adhere to the walls of the duct or it "separates"; a very undesirable phenomenon since energy losses result from the vortexing action and as a result the resistance to flow is greatly accentuated.

If the fluid is a liquid of sufficiently high vapor pressure, the static pressure near the inside wall of the duct may depress to a value equal to or below the vapor pressure and thus cause cavitation within the elbow which is an entirely different phenomenon from separation although both may occur simultaneously.

10
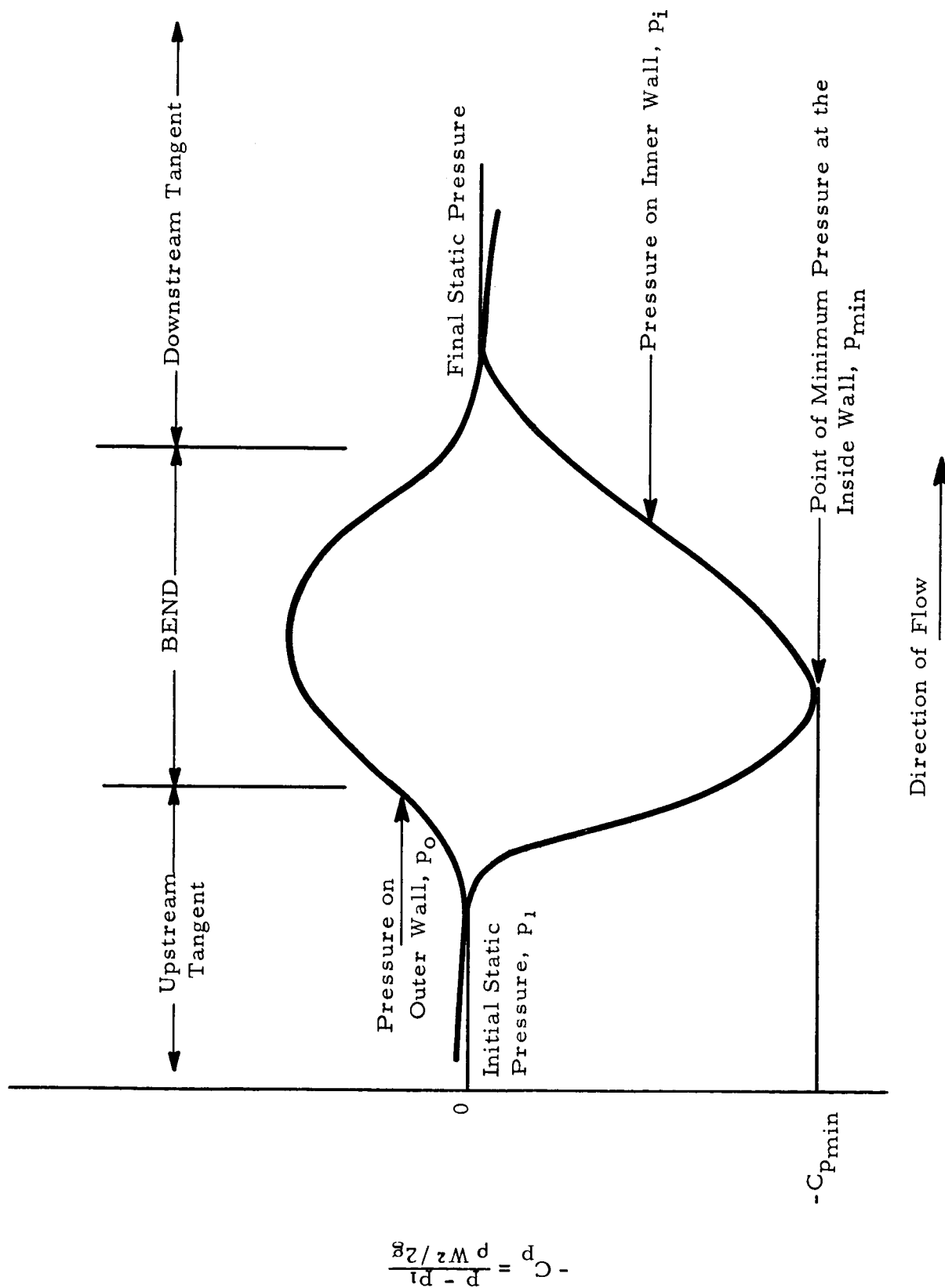
Figure 2. Schematic of the Pressure Distribution on the Inner and Outer Walls in the Plane of Curvature of an Elbow

$$-C_p = \frac{p - p_1}{\rho \, W^2 / 2g}$$

11

REVIEW OF EXPERIMENTAL CURVED FLOW RESEARCH

The discussion in this section is devoted primarily to experimental investigations of flow in curved ducts. The results and conclusions from these studies will be interpreted in such a manner as to describe the various features of the flow in regard to flow pattern distortions and pressure variations that arise from turning the flow.

Unfortunately, the bulk of the investigations performed to date have been directed towards experimentally measuring the loss coefficients with little regard for the nature of curved flow itself. Hopefully, the brief summary presented herein will serve as an introduction to the subject and will delineate and clarify the processes that govern the flow in curved pipes with a finite deflection angle and constant radius of curvature and flow area. Because of the inadequacy of data and the varied, and often unknown, conditions under which the studies were made, the phenomenological aspects of curved flow will be emphasized rather than the presentation of results for solutions for current developmental problems or for future design purposes.

A number of papers and reports are devoted to methods of controlling curved flow with such devices as turning vane cascades, changes in cross sectional shape and area, and others. While these techniques may eventually be employed as a solution to the present problems, studies of the individual characteristics of each configuration are devoted to a particular application and do not yield significant information on the basic nature of curved duct flow. In the interest of brevity, therefore, a discussion of these papers has regrettably been omitted but some of them are listed in the bibliography for those interested in further study.

In 1911 John Eustice[1] published the results of a study in which he injected dye at discrete points within a fluid stream entering a glass

12

elbow. By using six different colors of dye and with injection nozzles at various positions within the upstream straight section, the flow patterns could be observed as the flow progressed through the bend.

For the laminar flow conditions under which the study was conducted, it was observed that upon entering the bend some of the filaments of dye spread out into bands and crossed to the inner part of the tube. After reaching the inside of the bend the filament then reflected back across the tube but always remained in the half of the tube with respect to the plane of curvature in which the filament entered. Figure 3 is an attempt to illustrate some of the results obtained in this qualitative but fundamentally important investigation.

As the flow progressed through the bend, vortices were generated which persisted through the straight downstream pipe. Eustice concluded that the persistence of this vortexing, which increased the resistance to flow in the curved portion of the pipe, was also responsible for the increased resistance to flow in the straight pipe downstream of the turn. On increasing the flow velocity he found that the curvature of the stream lines also increased. Prior to the initiation of one test, a uniform coat of dye was spread on the inside of the pipe and when the water was allowed to flow the dye disappeared immediately from the outer wall of the bend, more slowly from the inner wall, and very slowly from the straight part of the tube. In this manner the variation of the shear stress at the tube walls was demonstrated.

G. I. Taylor[2] repeated some of Eustice's experiments with helical glass tubes, but in order to permit observation of the flow pattern in the elbow itself, Taylor introduced the dye into the stream after it had traversed at least one whole turn of the helix. Thus, any turbulence in the upstream tangent would not destroy the dye filaments before entering the coiled pipe.
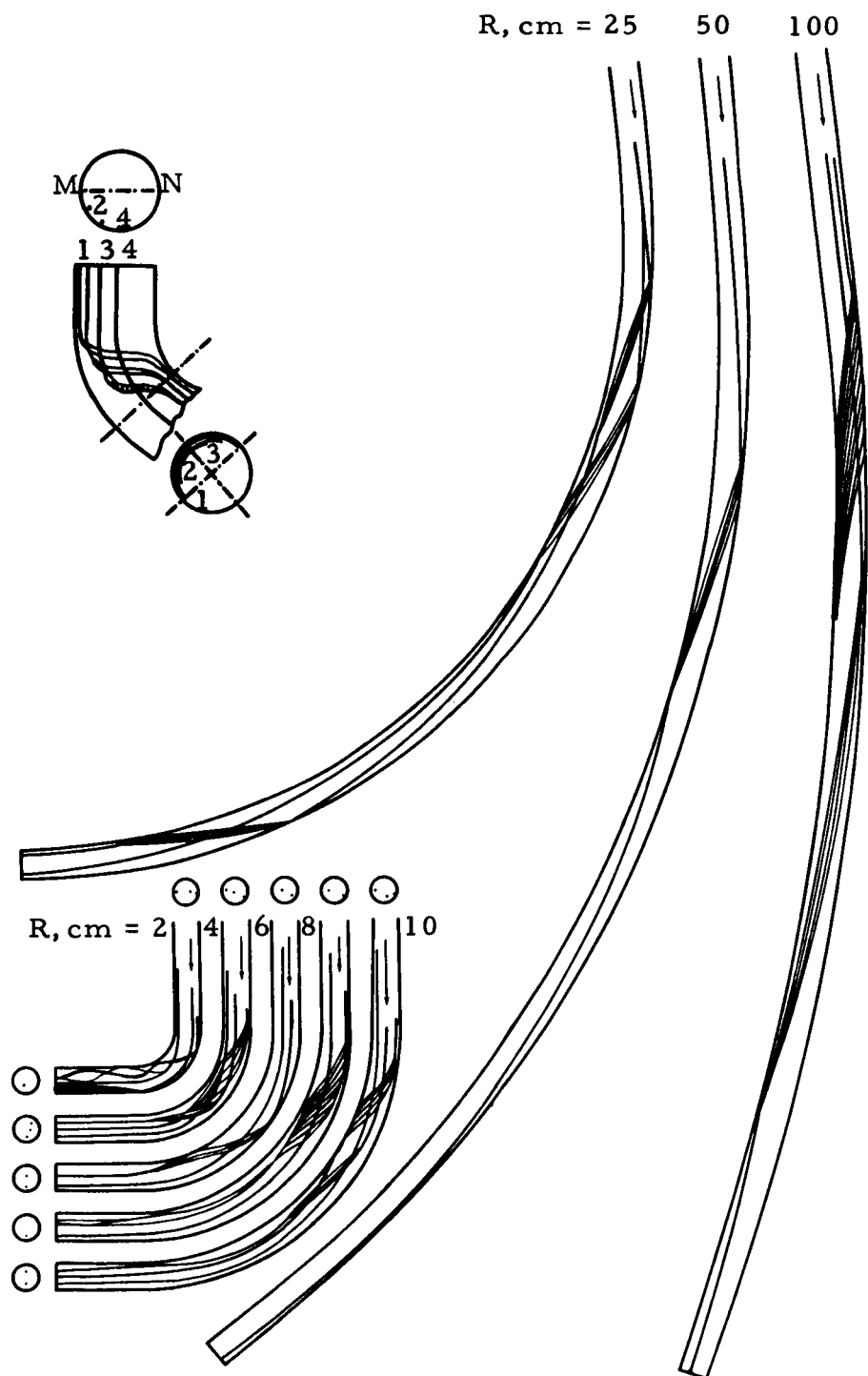
Figure 3. Trajectories of Dye Filaments Injected at the Entrance
to Curved Pipes (Reference 1)

14

Figure 4 is an illustration of the secondary flow processes Taylor found to be superimposed on the main flow. The dye, introduced at point A flows inwards along the wall until it reaches the innermost point B where it then leaves the wall and moves across the middle of the section to the outer-most point C. At point C the dye moves inwards along the wall again, thus completing the circuit. Occasionally, however, some of the dye divided at the point C and flowed towards point E.

Outside of Bend

Inside of Bend
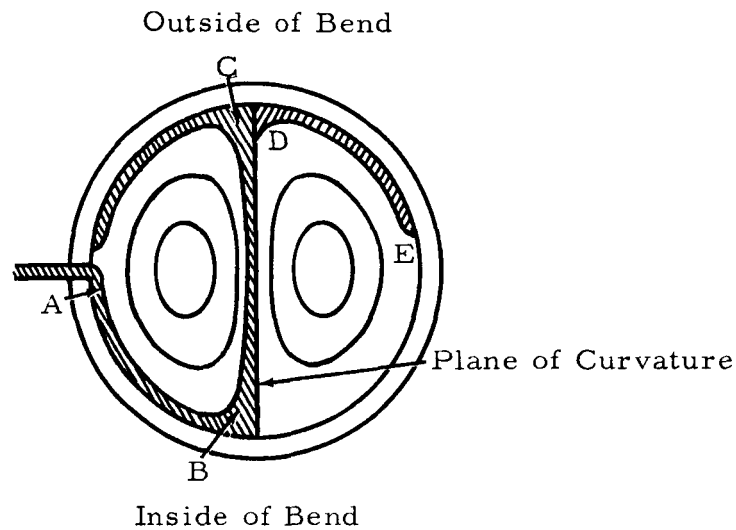
Figure 4   Circulation in the Cross Section of a Curved Pipe
(Reference 2)

Observations of the fluctuations indicated that there was a stabilizing influence on turbulence in curved flow, and transition did not occur until critical Reynolds numbers higher than those in a straight pipe were obtained. These visual studies directly supported the con-clusions of White[3] who deduced that the onset of turbulence was the reason that loss coefficients failed to be correlated by Dean's number, D, for laminar flow where

$$D = \frac{2\rho \, aW}{\mu} \left(\frac{a}{R}\right)^{\frac{1}{2}} \quad . \tag{9}$$

The loss coefficient, ζ, is defined as

$$\zeta \equiv \frac{\text{resistance coefficient of the curved pipe}}{\text{resistance coefficient of a straight pipe of same length and cross section}} \quad . \tag{10}$$

Figure 5 illustrates the variation of the loss coefficient, ζ, with D as presented by White. The points of departure of the individual curves from the main curve coincide with the onset of turbulence which occurs for

$$\frac{4\zeta \, \mu}{\rho \, a \, W} \leq 0.0045 \quad . \tag{11}$$

For the laminar flow case where ζ is correlated by D, White gives the following empirical relation for the loss coefficient

$$\zeta = \left\{ 1 - \left[1 - \left(\frac{11.6}{D}\right)^{0.45} \right]^{2.22} \right\}^{-1/0.45} \quad . \tag{12}$$

It must be emphasized that relative to the present interest in finite pipe bends, these results were obtained for coiled pipes wherein the flow has had an opportunity to become fully developed curvilinear flow.

On the basis of further studies, White concluded that if the entering flow is turbulent, the velocity profile will be flatter than for laminar flow and hence the pressure gradients across the bend will be less. As a result, the secondary flow processes are less pronounced and the losses are less influenced by curvature than for laminar flow.

Yarnell and Nagler[4] conducted a number of unique experiments with water in 6 inch diameter pipe bends. The most significant part of this work was the study of flow in the elbow and its downstream tangent when the velocity profile in the approaching pipe was varied from its normal uniform distribution about the pipe axis.
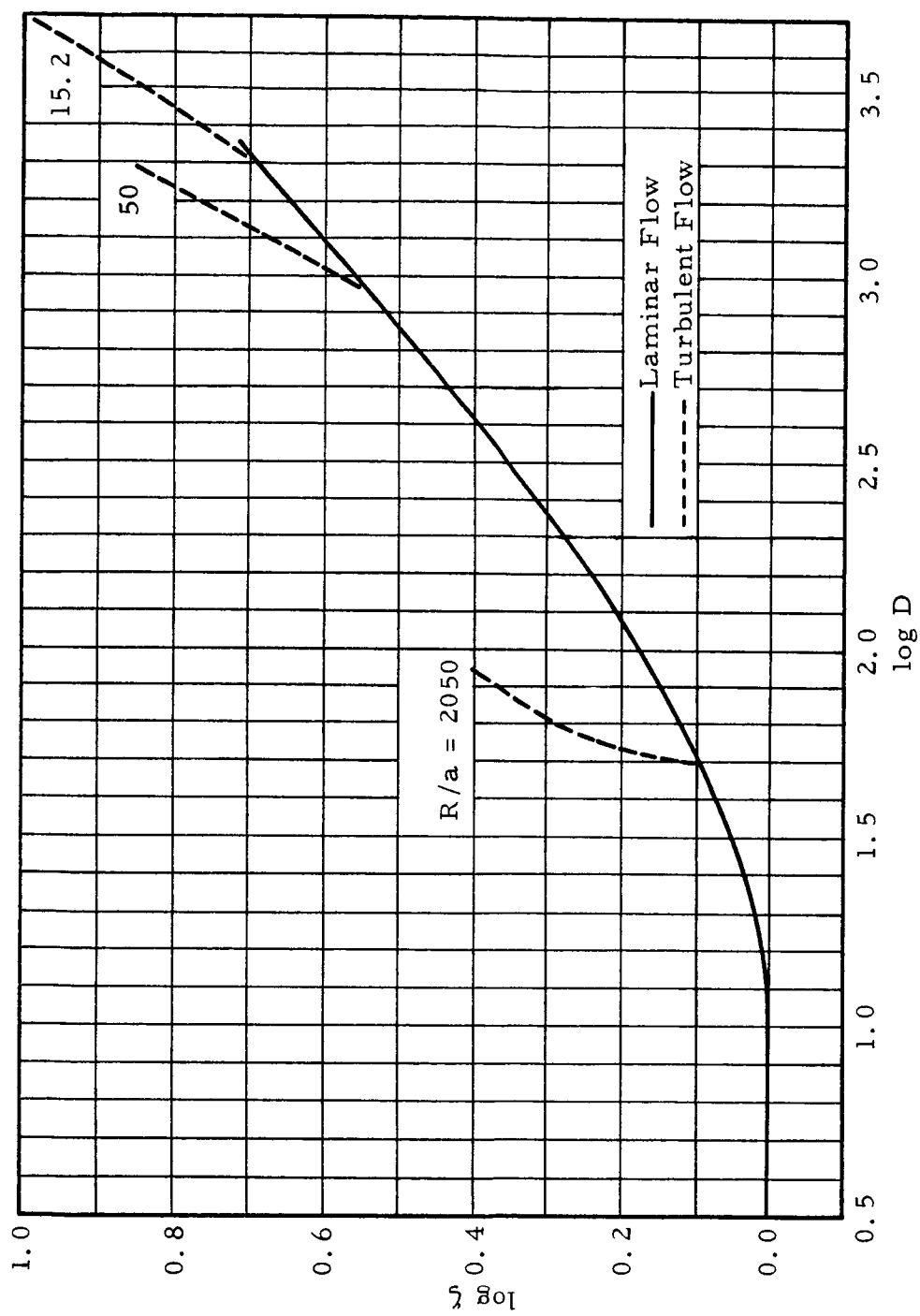
Figure 5. The Increase in Resistance Due to the Curvature of a Smooth Circular Pipe
(Reference 3)

17

Since the secondary flow processes in the elbow bend arise from the nonuniform velocity profile across the pipe at the entrance, the type of secondary current that prevails in a bend will depend on the nature of the velocity distribution in the approach tangent. Yarnell and Nagler found that if the particles of highest velocity are asymmetrically located with respect to the plane of curvature, rotation of the entire mass of fluid will be induced. If the high velocity particles are located above the plane of curvature, the secondary current will exhibit a counterclockwise motion as viewed looking downstream in a bend to the right. If the high velocity particles are located below the plane of curvature, the rotation is clockwise; i.e., the filaments of high velocity tend to rotate to the outside of the bend and the filaments of low velocity toward the inside of the bend when the velocity profile is asymmetrical with the plane of curvature. If the velocity distribution is symmetrical with respect to the plane of curvature, the two secondary currents of the type observed by Taylor[2] will be induced.

Figure 6 illustrates the influence of the asymmetrical entrance velocity profiles on the pressure distributions in the plane of curvature at the inner and outer walls of a 90° bend. Of importance to the cavitation tendencies of liquids in elbows is the change in minimum pressure at the inside wall as the velocity profile is distorted such that the high velocity is directed either to the outside or the inside of the entrance to the bend. With a symmetrical, fully developed profile at the entrance, the minimum pressure at the inside wall was about 2 feet of water. When the high velocity particles were directed to the inside of the bend entrance, the minimum pressure was about 2 1/2 ft; only about 1/2 ft below the pressure at the entrance. These results indicate that the cavitation characteristics of an elbow could be altered by imposing at the elbow entrance a nonuniform velocity profile with the high velocity directed towards the outer wall. From the data presented, velocity variations asymmetrical to the plane of symmetry apparently do not strongly influence the pressures on the inner and
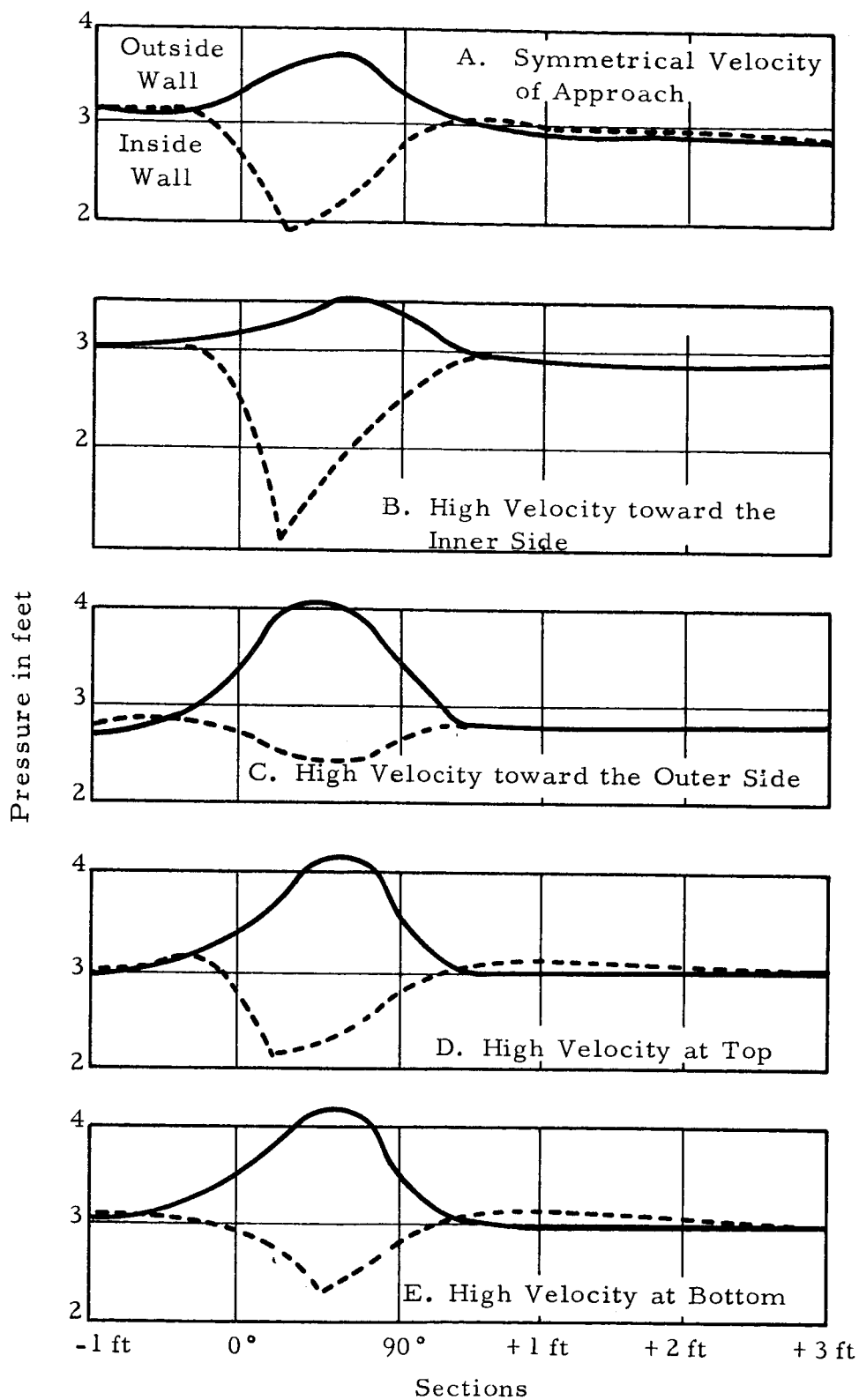
Figure 6. Pressures Along Inner and Outer Sides of 90° Bend with Various Velocity Distributions in Approach Channels. R/a = 2.84. (Reference 4)

19

outer walls although there seems to be some tendency to slightly increase the pressures on both the walls above that for symmetrical, fully developed flow at the entrance. However, these results do not imply that there is not a pressure decrease away from the walls.

The head losses measured in the downstream tangents also illustrate an important effect that nonuniformity of the entrance velocity profile may have on the flow downstream of the bend (Figure 7). Persistence of the flow distortions arising in the elbow may be inferred from the failure of the energy gradient in the downstream tangent to become parallel with the energy gradient for a straight pipe, e. g. , failure of the flow to quickly revert to fully developed pipe flow. The slowness with which fully developed pipe flow is obtained in the downstream tangent indicates the existence of secondary circulation which generates not only additional friction losses at the walls, but additional internal friction due to velocity gradients within the core of the fluid itself. The data illustrated by Figure 7 indicates intensive secondary circulation which persists far downstream of the bend especially when the velocity profile is asymmetrical with the plane of curvature. The entering velocity profiles that are symmetrical with the plane of curvature permit the flow to become fully developed in the straight section more quickly and hence indicate the generation of less severe secondary circulation in the bend itself. However, when the high velocity particles are initially directed towards the inside of the pipe, there is a considerable increase in head loss in the elbow itself, indicating quite possibly separation of the boundary layer at the inner wall due to the more extensive positive pressure gradient in the last 60° or so of the elbow. These results indirectly indicate that to avoid excessive flow distortion at the entrance to equipment located downstream of an elbow, one must use care in the design of the ducting components upstream of the bend, especially those that would tend to produce asymmetrical velocity profiles about the plane of curvature.

Figure 8 is an illustration of the isovels within the interior of a 90° bend and the static pressures about its periphery as measured by
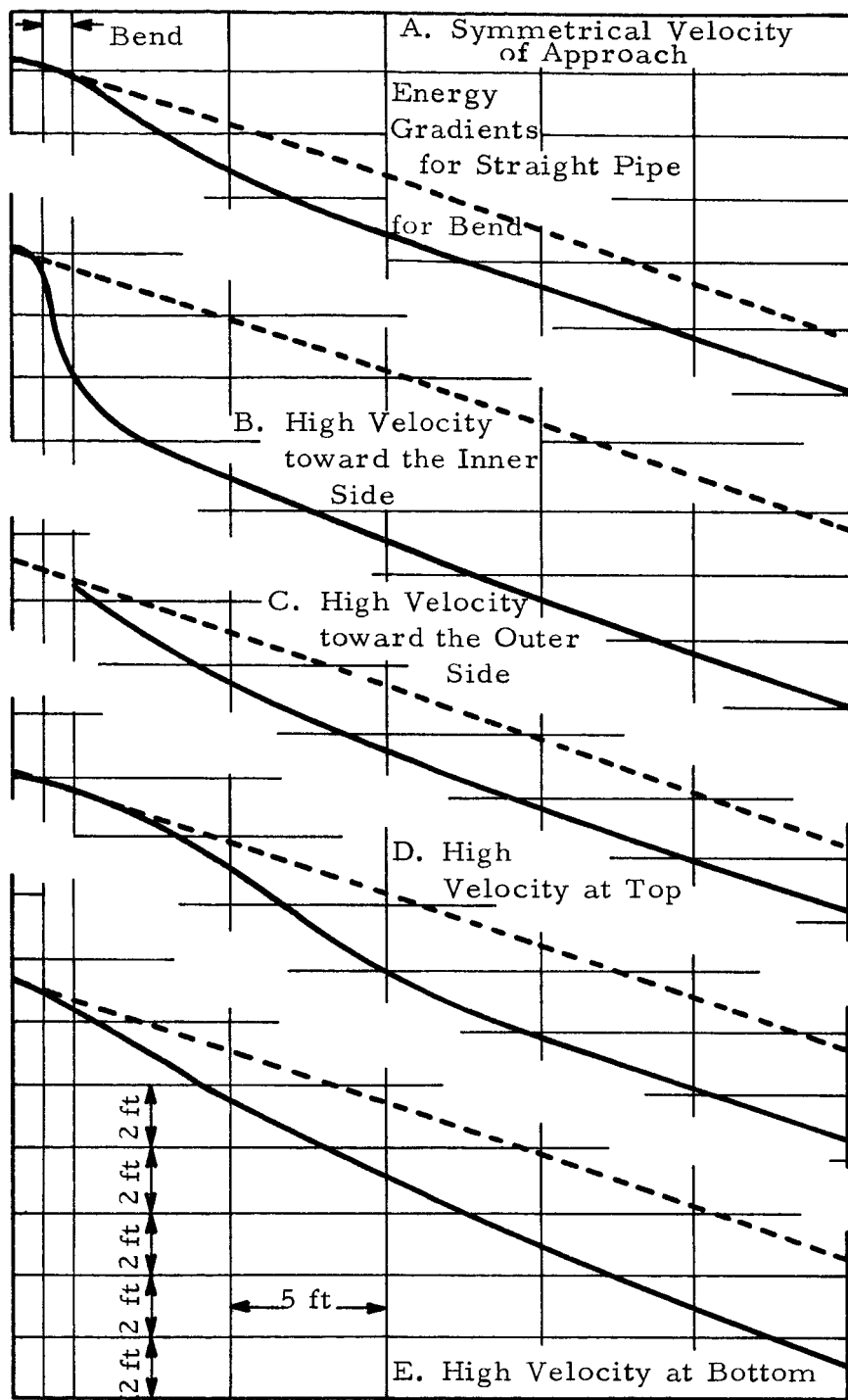
Figure 7. Head Loss in the Downstream Tangent
of 90° Bends for Different Inlet Velocity
Distributions. R/a = 2.84. (Reference 4)
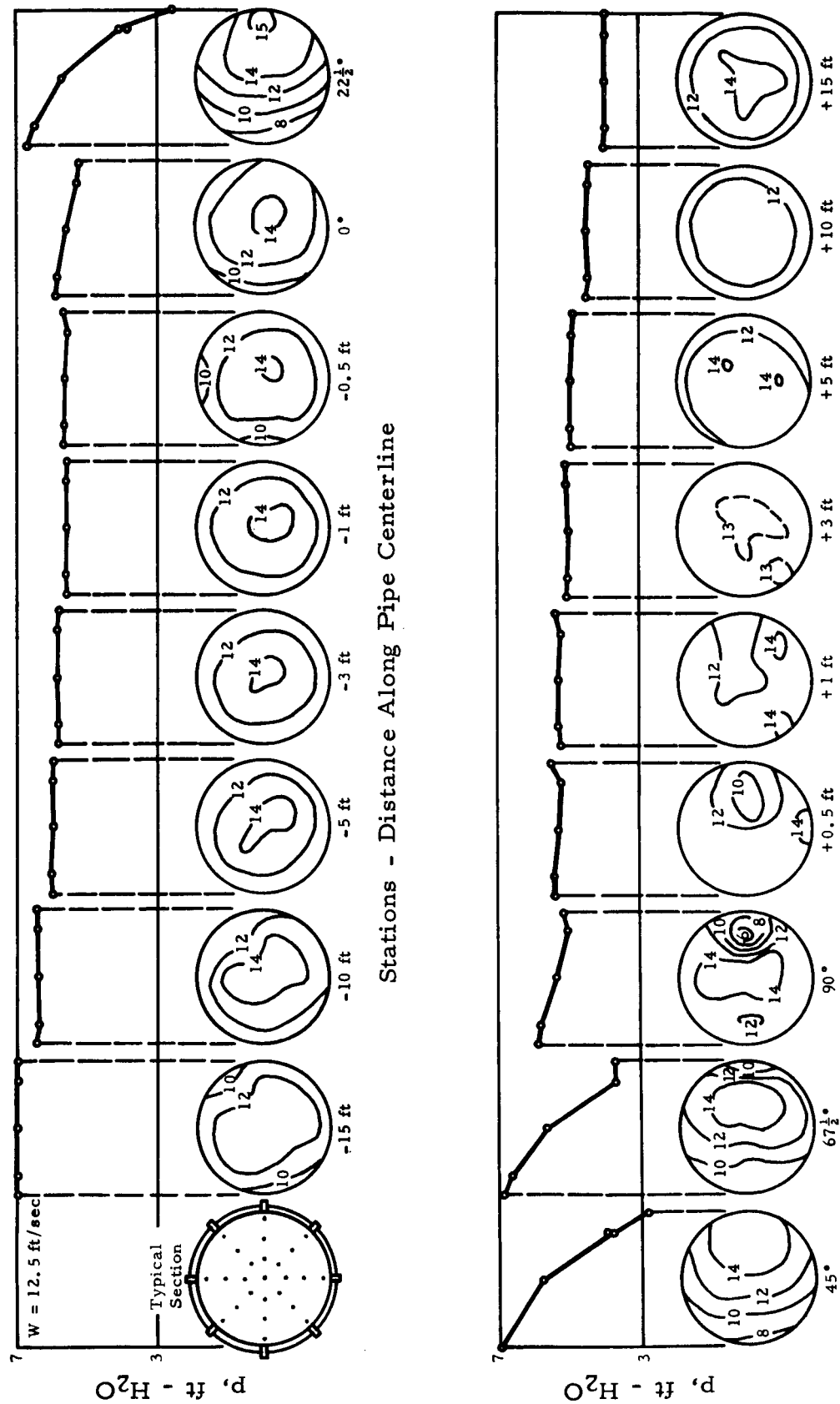
Figure 8. Velocity Distribution at Various Stations in a 90° Bend with Approximately Uniform Velocity Distribution in Approach Tangent - Transverse Profile of Pressure Shown Above Each Station (Reference 4)

22

Yarnell and Nagler. At the entrance (0°) the initially symmetrical
velocity distribution has already become influenced by the presence of
the elbow. The high speed filaments originally at the centerline of the
fully developed pipe flow begin to divert to the inside of the bend. Between
deflection angles of 0° and about 45°, this central core of high speed fluid
is not affected by viscosity and hence the secondary currents have not yet
developed. If it is assumed that the streamlines follow concentric circles
of radius r', then Euler's equations become

$$\frac{\partial p}{\partial r'} = \frac{\rho w'^2}{gr'} \tag{13}$$

where p is the static pressure, ρ is the density, and w' is the velocity
tangential to the pipe walls. If the flow is potential, then Bernoulli's
equation states

$$p + \frac{\rho w'^2}{2g} = P \tag{14}$$

where P is the total pressure and is a constant throughout the flow.
Differentiating Bernoulli's equation with respect to r', substituting into
Euler's equation and integrating gives

$$w' \, r' = K \tag{15}$$

which is the relationship between the tangential velocity and the streamline
radius of curvature for a potential vortex. Therefore, the tendency of the
high velocity streamlines to divert to the inside of the bend qualitatively
conforms to that predicted by potential theory.

As the flow proceeds further into the bend, past a deflection angle
of about 45 degrees for the measurements presented in Figure 8, the
developing secondary currents and viscous resistance begin to distort the
potential flow processes. The result being that the particles of maximum
velocity become displaced towards the outside of the bend by the secondary
currents which arise from the retarding action of viscosity near the walls.
These secondary currents are initially insignificant (especially for turbulent

23

flow) and confined to a narrow layer near the walls but they grow slowly in intensity and size with distance through the bend to eventually consume most or all of the potential flow. Since the formation of the secondary flow currents is dependent upon the amount of fluid contained in the viscous layer near the wall, the flow pattern of the entering fluid will exhibit a marked influence on the flow processes in the bend. The laminar velocity profile is approximately parabolic and hence much of the fluid may be considered to be entrained in a viscous layer. Turbulent flow, however, is governed primarily by turbulent mixing of the fluid rather than by molecular exchanges and hence the velocity profile is flatter near the center and steeper near the walls than the laminar flow. Consequently, the viscous layer of the turbulent flow is thinner than for the laminar flow and one may expect considerably different velocity profiles and pressure gradients in a pipe bend if this type of profile exists at the bend entrance.

Weske[5] has performed a number of experiments that illustrate many of the fundamental processes which govern the flow in curved pipes. He measured, in ducts of various cross-sectional shapes, the velocity and pressure profiles in 90° bends and downstream tangents. In a manner similar to that of Yarnell and Nagler[4], the effect of distorting the flow upstream of the bend was also studied. The tests were conducted using air instead of water as the working fluid and at velocities high enough to insure turbulent flow at the entrance to the bends and in some cases, separation of the flow at the inside wall.

On the basis of his measurements, Weske defines three distinctive regions of flow in curved ducts as follows (see Figure 9):

1. The "core" or central body of the fluid in which the velocity component in the axial direction is large compared to the transverse velocity components. In this region, the flow is largely unaffected by viscosity; thus, pressure and inertia forces predominate over viscous forces. The axial velocity distribution approximates free-vortex motion,

Direction of flow
in central body

Direction of flow
near wall

Velocity profile of velocity components in
cross-sectional plane

Station 1

Station 2

Station 3

Station 4

Region of
eddying motion

Region of
peripheral
flow

Central body
of fluid

Region of eddying motion

Station 1

Station 3

Station 4
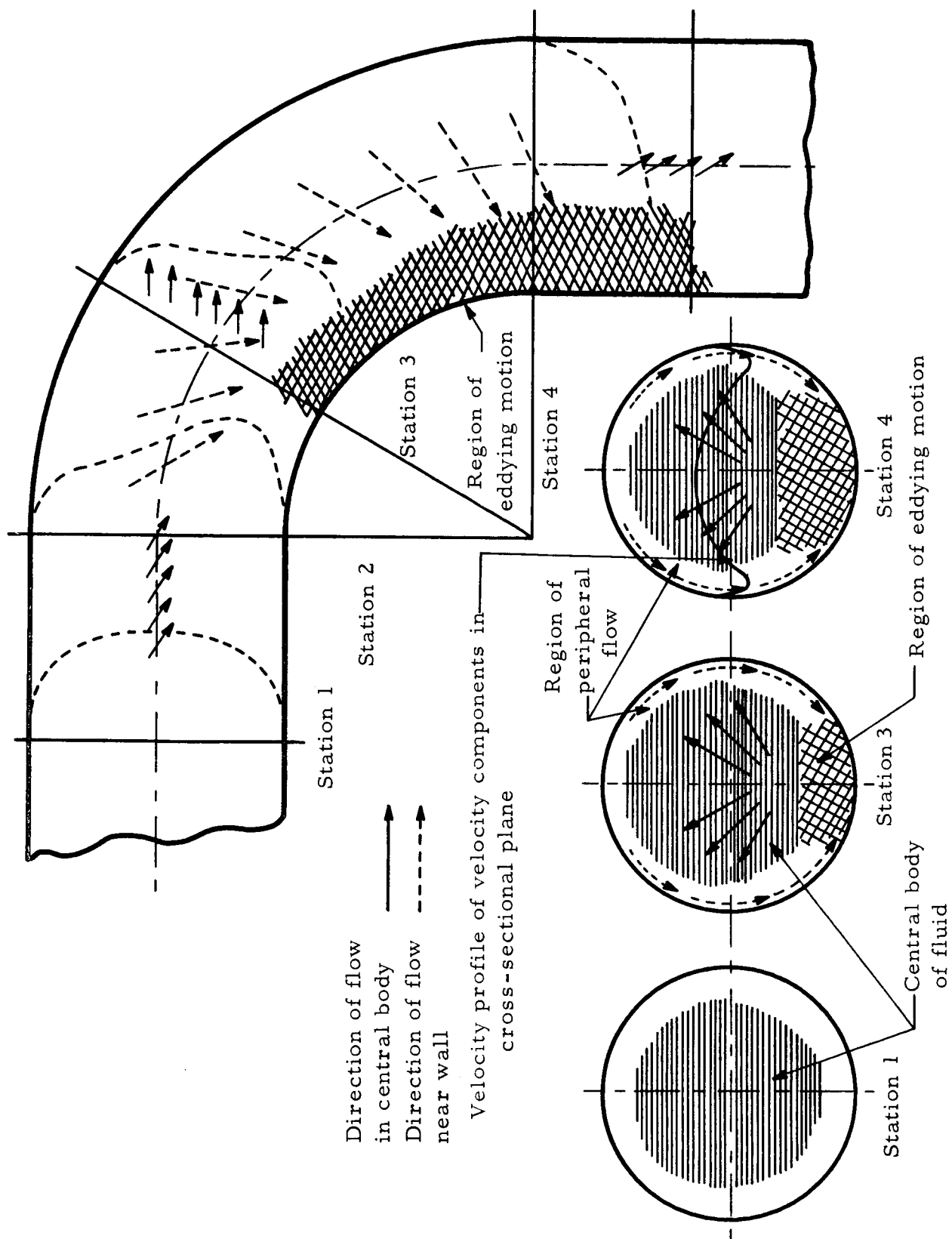
Figure 9.   Schematic Drawing Showing Flow Phenomena in a Curved Duct (Reference 5)

25

the product of radius and velocity being roughly constant across the section (Equation 15). As pointed out before, the portion of the flow contained in the "core" will vary according to the entrance velocity profile and distance through the bend.

2. The "shedding layer" near the wall in which the velocity component normal to the wall is near zero and the velocity component in the peripheral direction parallel to the wall is of the same order of magnitude as the component of velocity in the axial direction. The fluid in this layer has lost a large part of its kinetic energy through viscous stresses and it therefore flows towards the inside of the bend, in the direction of the negative peripheral pressure gradient imposed by the core flow. In many respects this "shedding layer" resembles the three dimensional boundary layer on the sweptback wings of high speed aircraft and on bodies of revolution immersed in a moving fluid and yawed with respect to the wind axis.

3. The "region of eddying flow" occurs at the inside of the bend where the opposing shedding layers impinge as they follow the curvature of the wall. In this region, the total energy of the flow is much less than in the core and the fluid is in a state of random turbulence. Distinction is made between eddy flow and separated flow which occurs when the radius of curvature is small. A complete reversal of flow arises in the latter case when the viscous layer at the inner wall lacks sufficient momentum to penetrate the region of positive axial pressure gradient near the bend exit.

By careful measurements with directional pitot-tubes and hot-wire anemometers, Weske obtained the velocity distributions in curved ducts, one of which is illustrated for a circular cross sectional shape in Figure 10 along with the total and static pressure measurements in the plane of the curvature. The potential flow approximation (Equation 14) is seen to be valid since the total pressure is essentially constant throughout the main body of the flow, the notable exception being near the inside wall in the eddy flow region where it is much lower. The static pressure increases

26

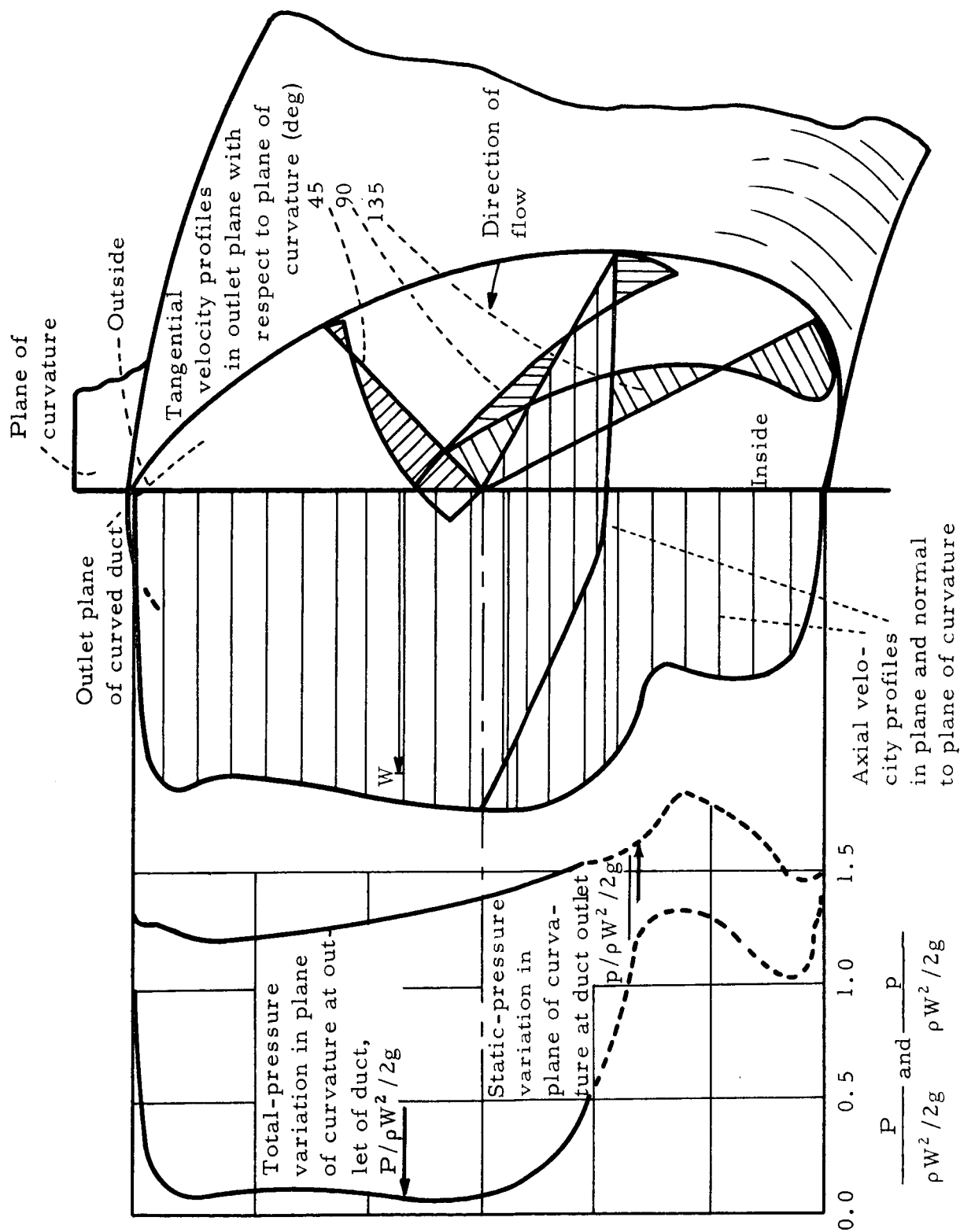Figure 10. Velocity Distribution at Outlet of a 90° 6-Inch-Diameter Elbow, $R/a = 3.0$, Reynolds Number $= 0.605 \times 10^{6}$. Velocities Plotted as a Fraction of Mean Velocity, W. (Reference 5)

uniformly from the inner wall to the outer wall as required to maintain equilibrium with the centrifugal forces. The axial component of velocity in the plane of curvature indicates a distribution approximating the potential flow; that is, $wr' = $ constant, with the exception of a small portion near the outside wall in the shedding layer and a much larger portion near the inside wall in the region of eddy flow. The axial velocity profile in the plane normal to the plane of curvature was similar to that in a straight duct. The profile of the velocity component tangential to the wall reveals the inward motion of the fluid in the shedding layer near the wall and a region of outwardly directed fluid in the central core as required to conserve mass.

Axial velocity measurements in a number of diametral planes are presented in Figure 11. These measurements illustrate the region of eddying flow which extends across the cross-sectional area from the inner wall to approximately along a line normal to the plane of curvature. The pressure profiles in these planes are presented in Figure 12. An important feature of the static pressure survey is that the pressure conforms to potential flow expectations since, for the most part, it is essentially linear with radial distance from the duct centerline in all the planes except the one normal to the plane of curvature and in this one it is almost a constant. As in the previous illustrations of the flow variables, the pressure in the region of eddy flow exhibits a behavior considerably different from that in the remainder of the duct cross section; thus, pressure is observed to reach its minimum value not at the inside duct wall but at some distance away external to the eddy flow region.

The velocity and static pressure measurements obtained in the midplane of curvature at various stations in the tangent downstream of a 90° elbow are presented in Figure 13. For the conditions under which the measurements were made, transition to fully developed pipe flow appears to be taking place at the distance of 12.3 diameters from the elbow outlet. These results are comparable to those of Yarnell and Nagler[4] in Figure 7, taken with water under very similar flow conditions, which indicates from

28
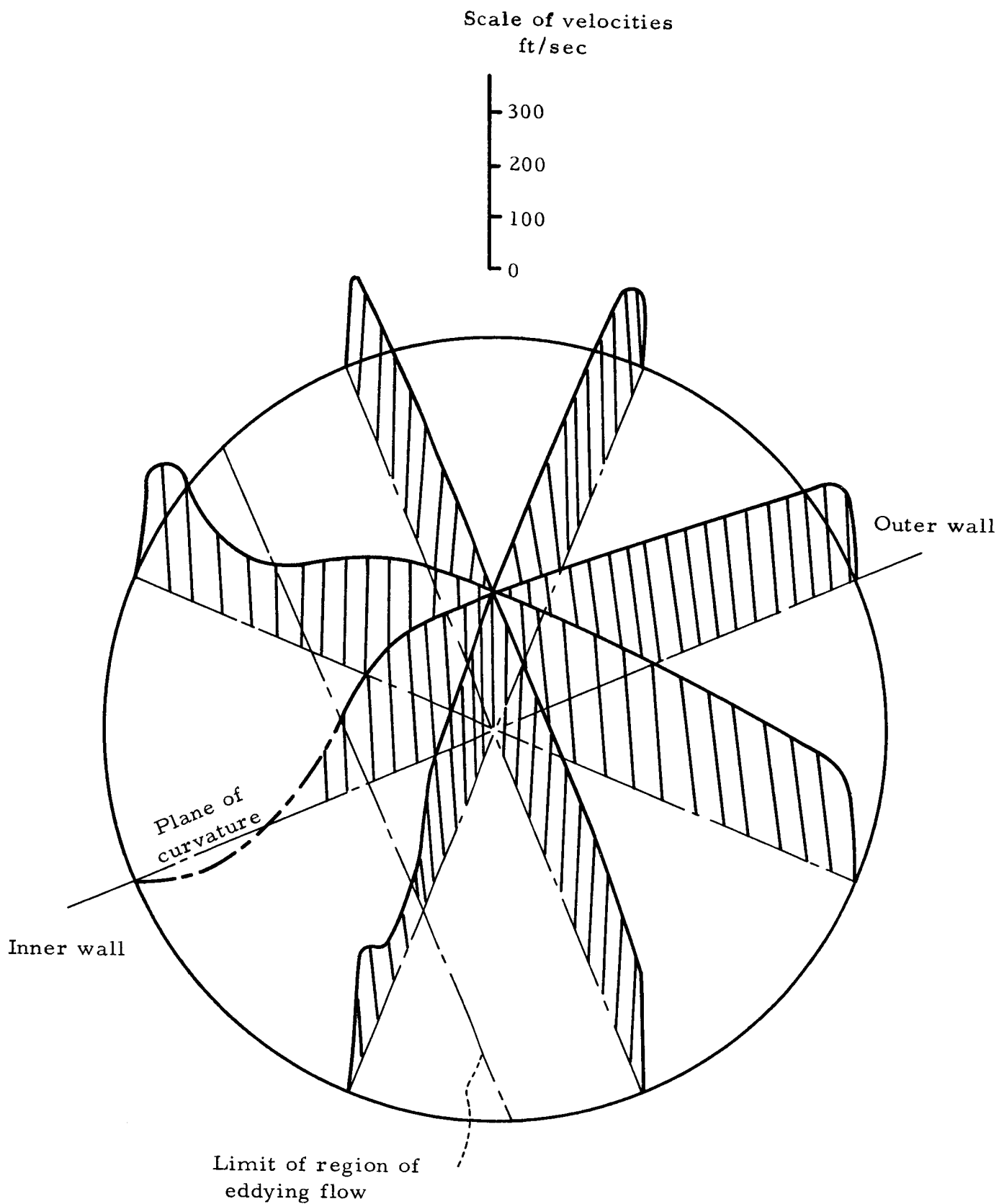
Figure 11. Axial Velocity Distribution at Outlet of 6-Inch-Diameter, 90° Elbow. R/a = 1.5, Reynolds Number = 0.535×10^6. (Reference 5)

Figure 12. Static-Pressure Distribution at Outlet of
6-Inch Diameter, 90° Elbow. R/a = 1.5,
Reynolds Number = 0.535 × 10⁶. (Reference 5)

30
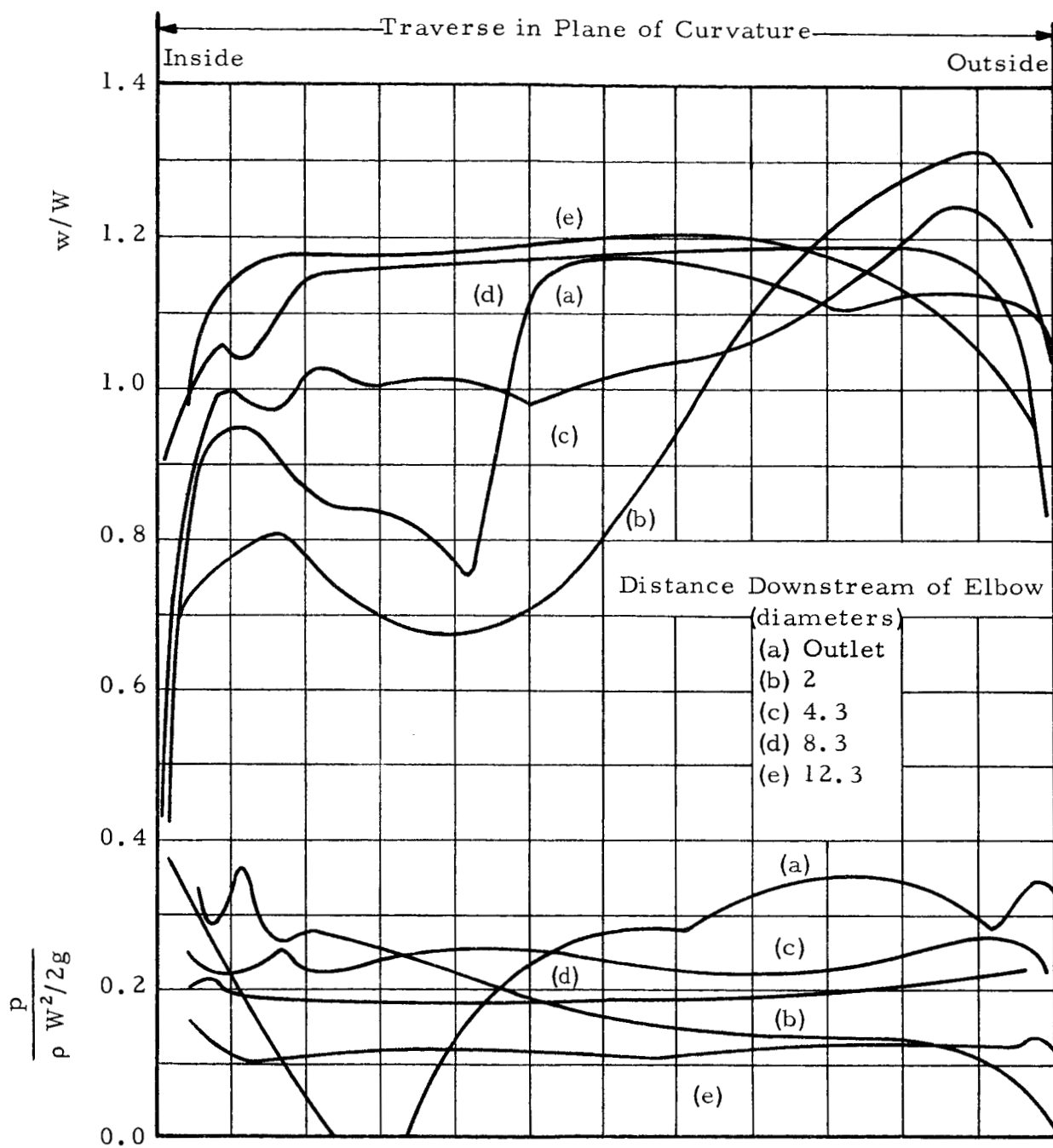
Figure 13. Velocity and Static-Pressure Traverse in Plane of Curvature
at Various Distances Downstream of a 90° Elbow of Circular
Cross Section 6 Inches in Diameter. R/a = 3.0, Reynolds
Number = 0.304×10^6. (Reference 5)

the slope of the head loss curve that fully developed pipe flow has been achieved in about 20 diameters from the elbow exit. The increase in static pressure at the inside of the pipe at two diameters indicates an impingement of the fluid at the inner wall such as was observed by Eustice[1] and illustrated in Figure 3. Weske tentatively concludes from Figure 13 that at 2 diameters from the bend outlet, "the main mass of fluid, performing a motion of two spirals symmetric with respect to the plane of curvature, is displaced toward either side, the region near the plane of curvature being occupied by eddying fluid surging up from the region of the inside wall of the duct". It would have been interesting and perhaps enlightening if Weske has presented measurements from traverses in diametral planes other than in the plane of curvature.

The effect of asymmetrical variation of upstream velocity profiles on the downstream flow is illustrated in Figure 14. Curves (a) and (c) present the axial velocity profile in the plane of curvature at the elbow outlet when the screen, by which the velocities in one half of the duct were reduced, was placed on the inside and on the outside respectively of the elbow inlet duct. These profiles are not too different from the profile (b) produced by symmetrical entrance velocity. However, Yarnell and Nagler, by their head loss measurements under similar circumstances, (Figure 7) indicate a marked difference in the nature of the flow in the downstream tangent when the screen is on the outside rather than on the side or when the flow is initially uniform.

The velocity measurements downstream of the elbow when the screen is placed on one side of the plane of curvature (curves d, e, f, and g), indicate a pronounced rotary motion such that the fluid of higher velocity spirals in the duct appearing first on one side of the duct and then on the other until the fluid of higher kinetic energy is rather uniformly distributed around the circumference and enclosing the fluid of lower kinetic energy near the duct centerline. These measurements substantiate the inference from Yarnell and Nagler's head loss measurements (Figure 7) that there

Figure 14. Effect of Unsymmetries Upstream Upon Velocity
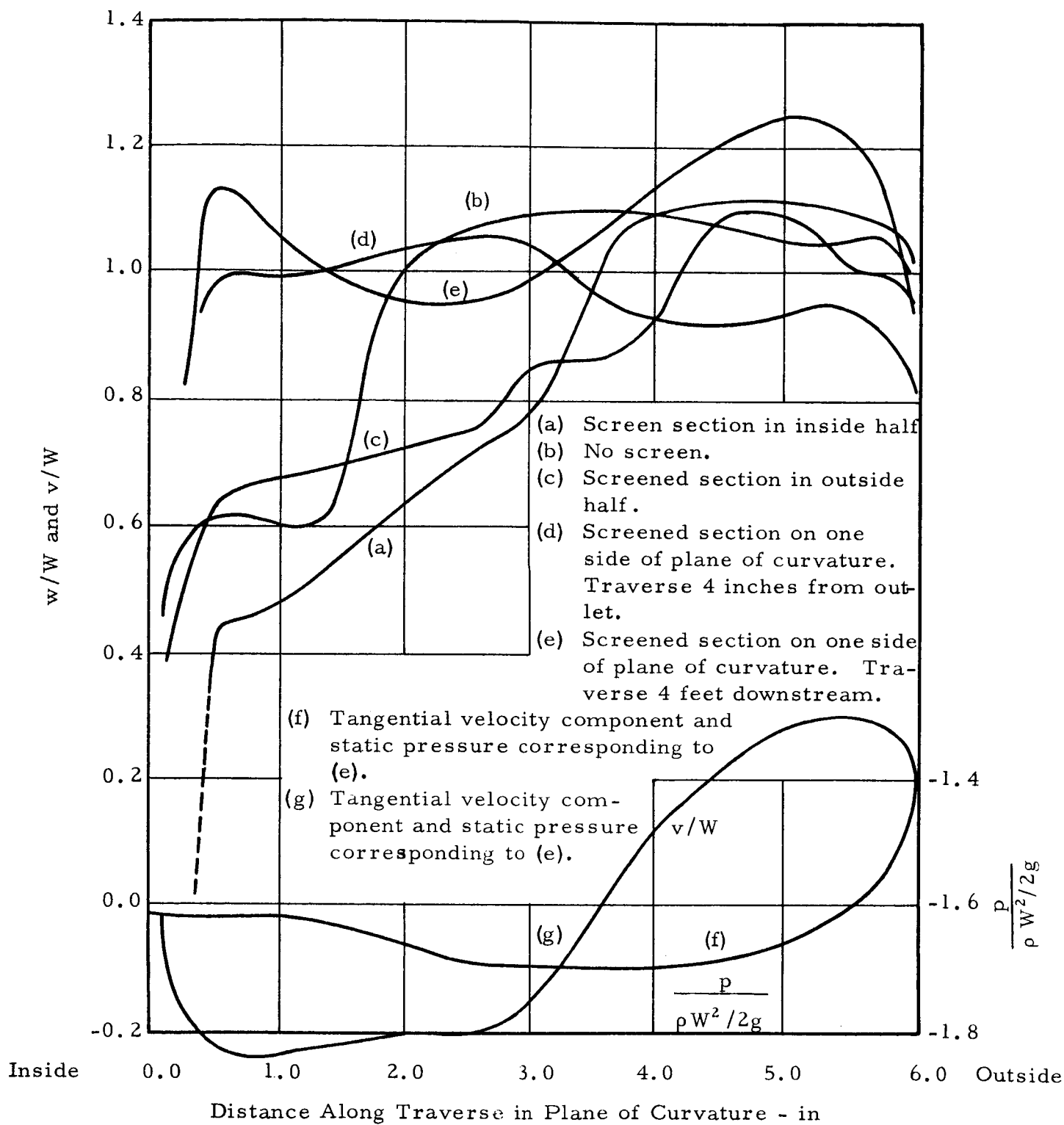Distribution in a 6-Inch-Diameter, 90° Elbow.
R/a = 3.0, Reynolds Number = 0.3 × 10^6.
(Reference 5)

is considerable distortion of the flow in the downstream tangent when the entrance velocity profile is asymmetrical with respect to the plane of curvature. As Figure 7 indicates, this latter condition persists for many diameters downstream from the bend and requires a much longer transition length to attain fully developed pipe flow than for the other cases studied. The motion from this type of entrance velocity profile arises from the asymmetry of centrifugal forces about the plane of curvature; the fluid of greater total energy having the largest centrifugal force exerted on it. The unbalance of force tends to rotate the entire mass of fluid around the duct axis so that the particles of higher total energy move to the outside of the bend and the particles of lower total energy to the inside. Because of angular momentum developed, the rotation continues until the particles of higher total energy have rotated approximately π radians from their original positions, then the cycle repeats itself with the rotation in the opposite direction. If the elbow deflection angle is not too great, the cyclic motion will persist a great distance downstream of the bend until it decays from viscous forces in a manner not unlike the motion of a damped pendulum.

Using an inviscid fluid theory, Hawthorne[6] derived, to the first approximation, the relationship for the angular displacement of the streamline pattern with the angle of bend deflection for a linear velocity profile at the bend entrance, the fluid particles of highest velocity being located at the top of the pipe. Figure 15 presents the relationship that Hawthorne developed and illustrates the analogy of fluid oscillation with the motion of a pendulum indicating the type of rotational motion that occurs (both experimentally and analytically from such an entrance velocity profile).

Presumably, it was a similar type of motion that induced the oscillations that Eustice and Weske observed with a symmetrical entrance velocity profile. With the symmetrical velocity profile, however, there would be two axes of rotation displaced on either side of the plane of curvature and roughly parallel to the axis of the duct. The fluid would
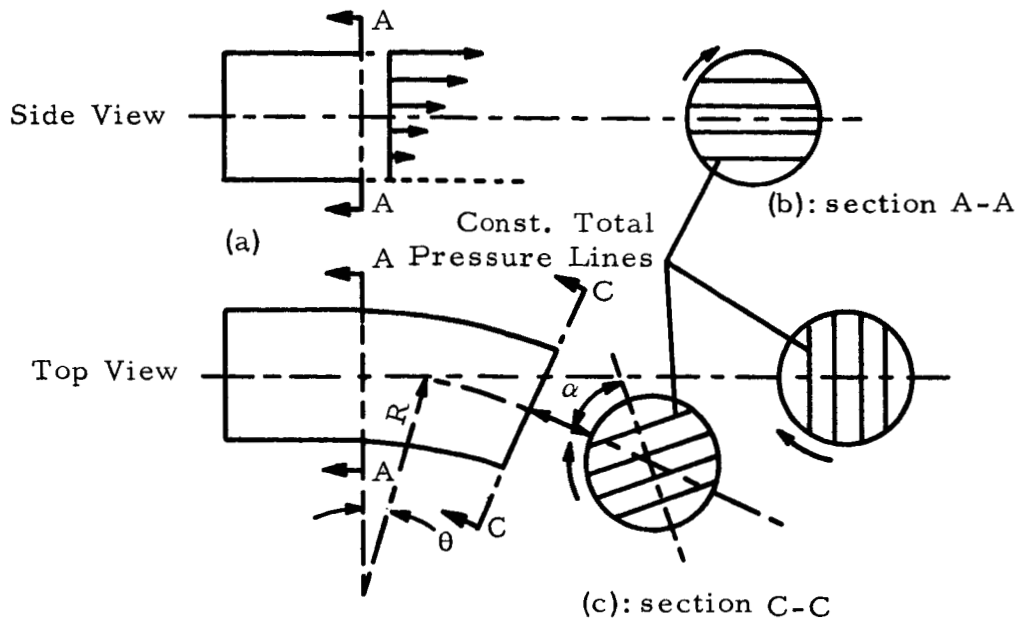
A. The Effect of a Bend on Flow with a Linear Velocity Gradient at the Entrance. (a) Surfaces of Constant Total Pressure at the Entrance. (c) Rotation of the surfaces through angle α.

Pendulum Geometry

Pendulum

$$\frac{\ell \, d^2 \alpha}{g \, dt^2} = \cos \alpha$$

$$\text{period} \simeq 2\pi \sqrt{\frac{\ell}{g}}$$

Secondary Circulation

$$\frac{2}{R/a} \cdot \frac{d^2 \alpha}{d\theta^2} = \cos \alpha$$

$$\text{period} \simeq 2\pi \sqrt{\frac{2}{R/a}}$$
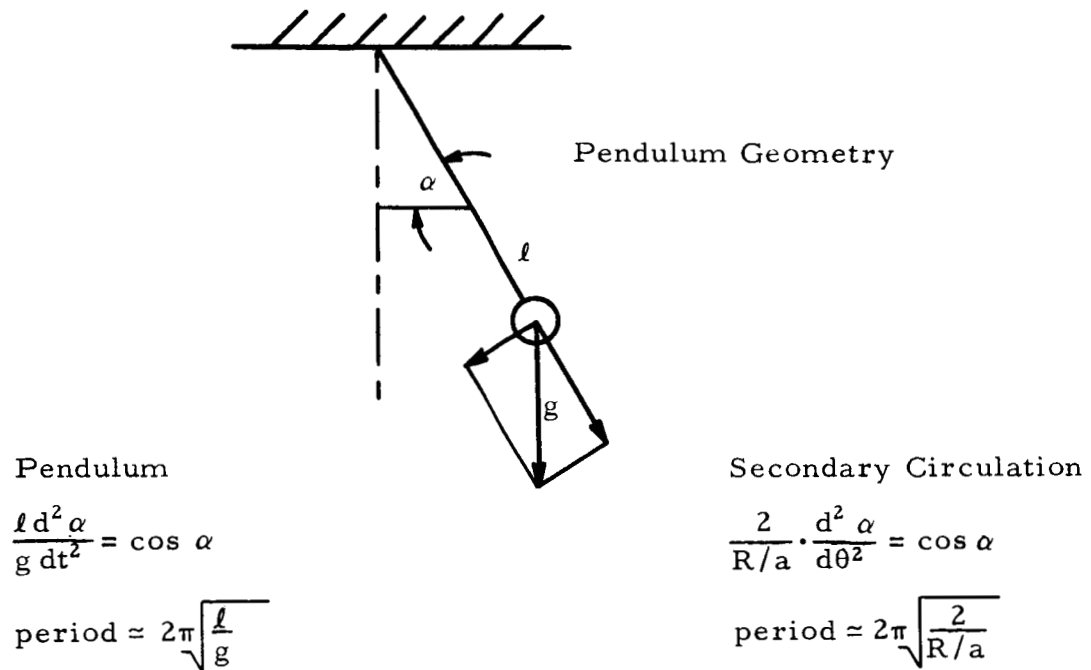
B. Analogy Between the Secondary Circulation and the Motion of a Pendulum.

Figure 15. Analysis of Secondary Rotation in a Curved Pipe (Reference 6)

tend to rotate in two spirals about each of the two axes (as illustrated in Figure 15 for the linear velocity profile); the particles of highest velocity originally at the duct axis moving to the outside of the bend. Rotation about the two secondary axes would continue until the low and high velocity regions have almost exchanged positions as indicated by Weske's measurements and the motion would then reverse itself to repeat the process in the opposite rotational direction to give the dampened oscillations of the fluid across the downstream tangent. These processes are very subtle and difficult to measure because of rapid frictional dampening and because they are superimposed on the more discernable axial motion.

As was illustrated in the data of Yarnell and Nagler and of Weske, the flow conditions in the downstream tangent are strongly affected by the flow conditions at the exit of the elbow. Variations in these exit conditions were achieved by distorting the velocity profile at the entrance to the bend. It would be of interest, however, to experimentally determine the effects on the flow in the downstream tangent of the oscillatory processes just described for a symmetrical entrance velocity profile by allowing the flow to exit the elbow at different points in its rotational cycle. Martin and Deverson[7] performed such an investigation by conducting a series of total head traverses at various deflection angles in the plane of the bend of a three-coil helical pipe and then determining the position of the particles of maximum total pressure as a function of the bend deflection angle θ. Figure 16 illustrates the oscillatory motion of these particles and the rapid dampening from the viscous stresses. After the flow has traversed about 360° through the coil, the oscillations are completely damped and the transition from rectilinear flow to fully developed curvilinear flow has taken place wherein the velocity profiles remain unchanged with deflection angle θ as the flow progresses further through the coiled pipe. From the relationship shown in Figure 16, the bend deflection required for a complete oscillation of the secondary current was determined to be 195°. The
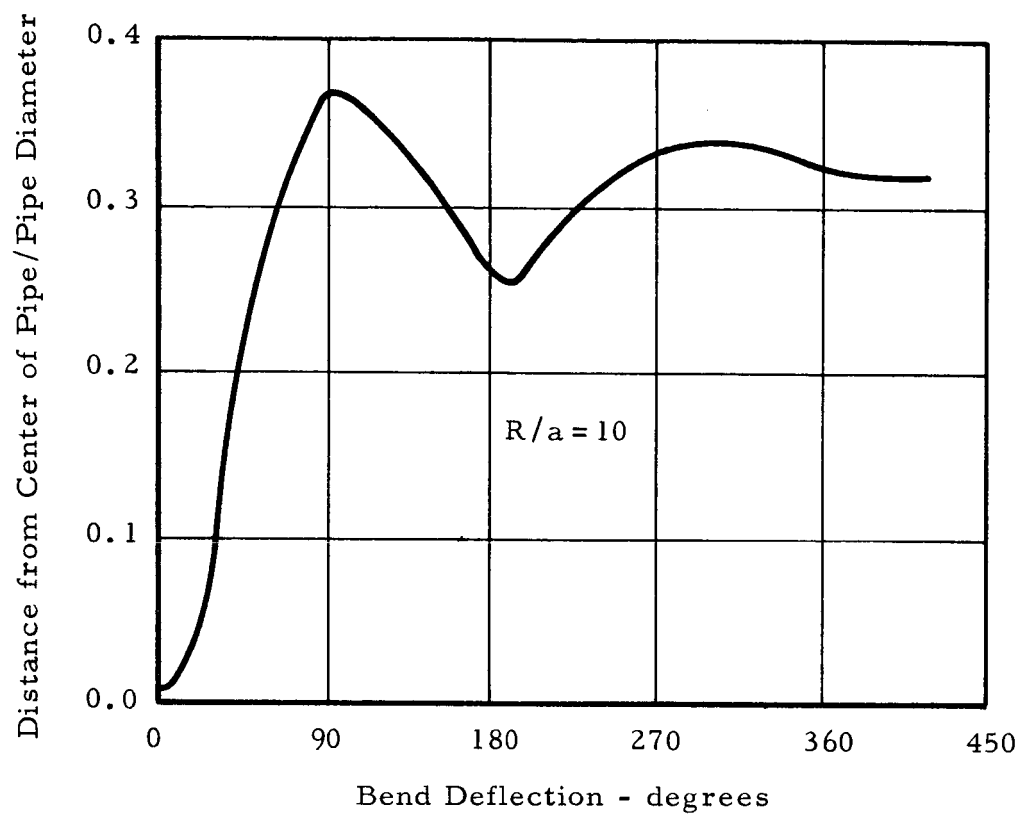
Figure 16. Position of Particles with Maximum
Total Pressure in a Helical Coil
(Reference 7)

37

general relation for the period of oscillation (Figure 15) for the conditions of these measurements would be

$$\text{Period} = (1.21)(2\pi)\left(\frac{2}{R/a}\right)^{\frac{1}{2}} . \qquad (16)$$

The secondary circulation in the bend will be a maximum after a quarter period of oscillation which would be the bend deflection angle at which the particles of maximum total pressure impinge on the outer wall. For the particular conditions studied, the deflection angle at which maximum circulation occurs is

$$\theta_m = \frac{1.21\,\pi}{2}\left(\frac{2}{R/a}\right)^{\frac{1}{2}} . \qquad (17)$$

A 30° bend was formed with the $\frac{2}{R/a}$ ratio calculated from the above equation to give maximum circulation at the bend outlet. The same value of $\frac{2}{R/a}$ will produce zero secondary circulation at the outlet of a 60° bend when the particles of maximum total pressure have rotated approximately 90° around the axes of secondary circulation and a small circulation in the opposite direction at a bend deflection angle of 70°.

Figure 17 shows the total pressure traverses made in and normal to the plane of curvature at various deflection angles in the 30° bend and at different stations in the downstream tangent. The continued displacement of the location of maximum total pressure toward the outside wall in the bend and downstream tangent indicate the existence of strong secondary vorticity at the bend outlet as was predicted by the theory. The rotary motion persists far downstream of the bend outlet with the tendency for the particles of highest stagnation pressure to become uniformly distributed around the circumference of the pipe and enclosing the fluid of lower kinetic energy near the duct centerline; these findings conforming to those of Weske. Even at 71 diameters from the bend outlet, the total pressure profile is not exactly symmetrical, indicating that fully developed pipe flow has not been attained.

38
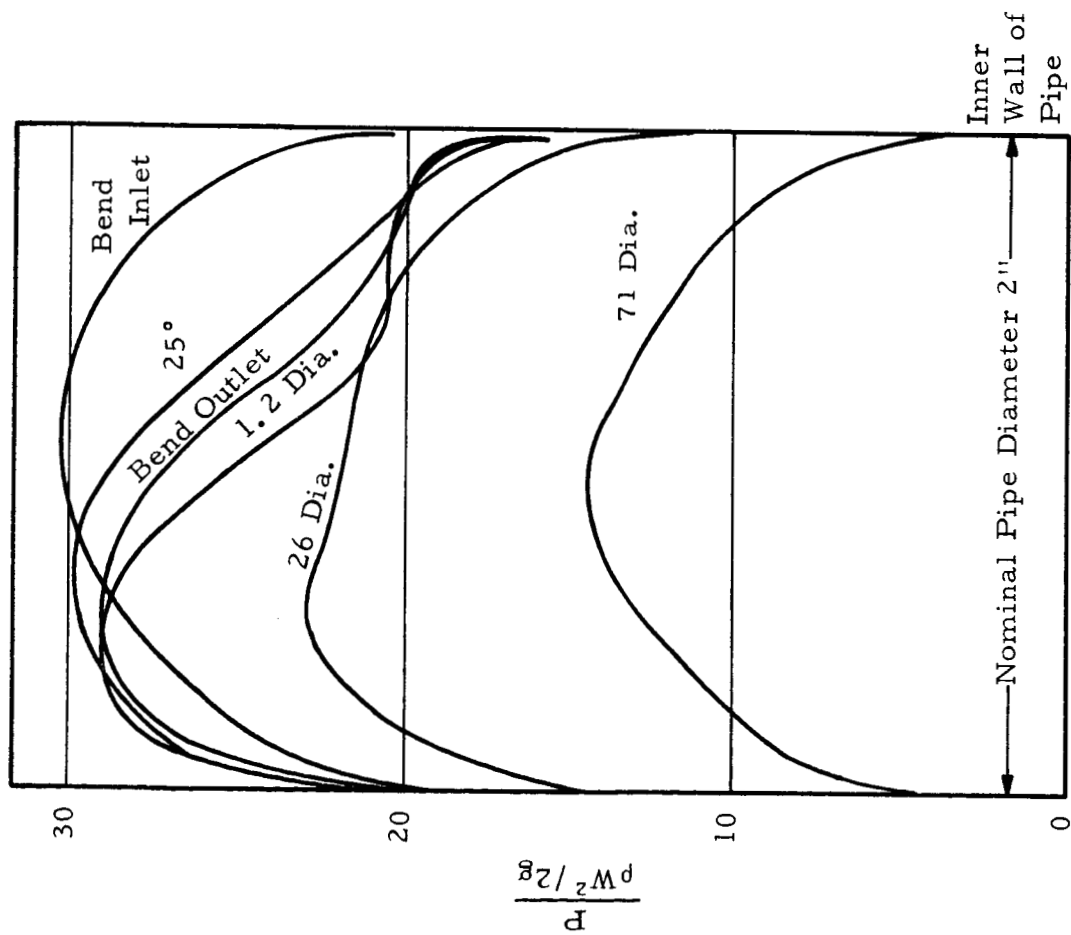
(a) Total Pressure Profiles Across Centerline of Pipe in Plane of Bend
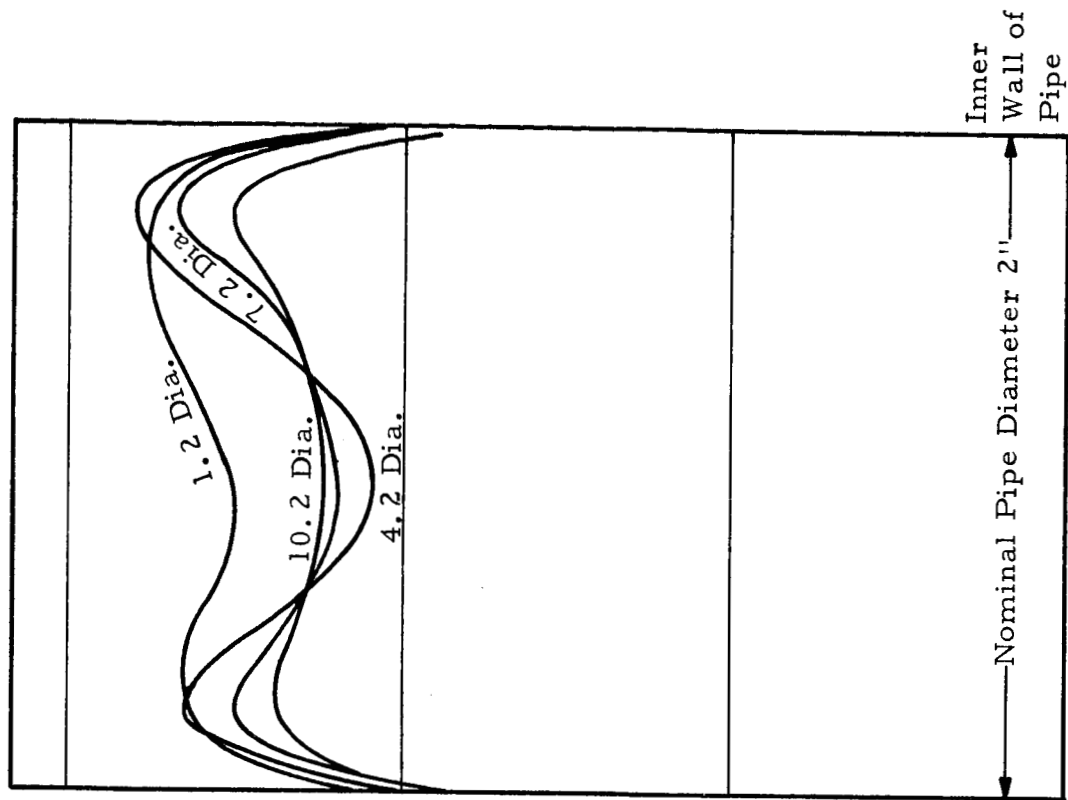
(b) Total Pressure Profiles in Plane Normal to Plane of Bend

Figure 17. Total Pressure Profiles in a 30° Bend and Downstream Tangent (Reference 7)

39

Figures 18 and 19 illustrate the total pressure profiles in the plane of the 60° and 70° bends at the bend outlet and several different stations in the downstream tangent. Once again, as was predicted by theory, the point of maximum total pressure in the 60° bend retains its relative position with the outside wall at various stations in the downstream tangent indicating no rotation of the fluid, but for the 70° bend the point moves away from the wall indicating a secondary rotation in the angular direction opposite from that in the 30° bend. From the total pressure profiles, it is observed that uniform pipe flow was attained more rapidly, in about 60 diameters, than for the 30° bend.

Another investigation was conducted by Martin and Deverson to examine the effect of shortening the downstream tangent less than that required to achieve fully developed pipe flow. Figure 20 presents the total pressure traverses made in the plane of the bend at the outlet of the 70° elbow as the downstream tangent was successively shortened. It was observed that on the inside of the bend there is a pressure maximum which diminishes as the tangent is shortened until it disappears if the tangent length is zero. Conversely, while the maximum at the inner wall disappears with decreasing tangent length, the total pressure maximum at the outer wall becomes more pronounced. Furthermore, as indicated by the total pressure readings near the walls where the velocity is essentially zero, the static pressure in the bend decreases with diminishing downstream tangent length.

These results of Weske and of Martin and Deverson are especially significant when applied to the design of a ducting system of circular cross sectional shape if turbomachinery is to be located downstream of a pipe bend or to the proper interpretation of measurements made within the bend itself. As predicted by theory and qualitatively confirmed by experimental data, the relationship between the bend radius of curvature and its deflection angle which would give the most uniform flow conditions at the outlet in terms of minimized secondary rotation is
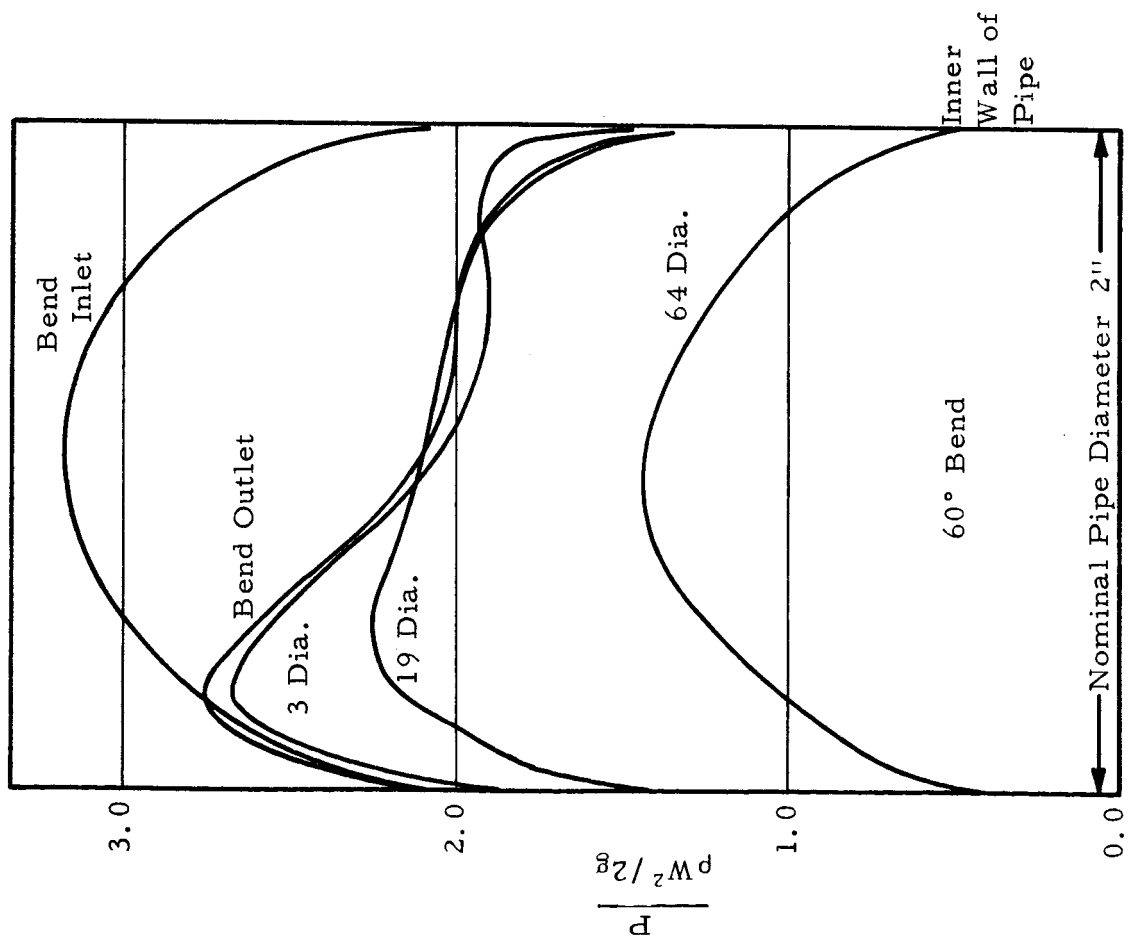
Figure 19. Total Pressure Profiles in Plane of Bend (Reference 7)

Figure 18. Total Pressure Profiles in Plane of Bend (Reference 7)

41
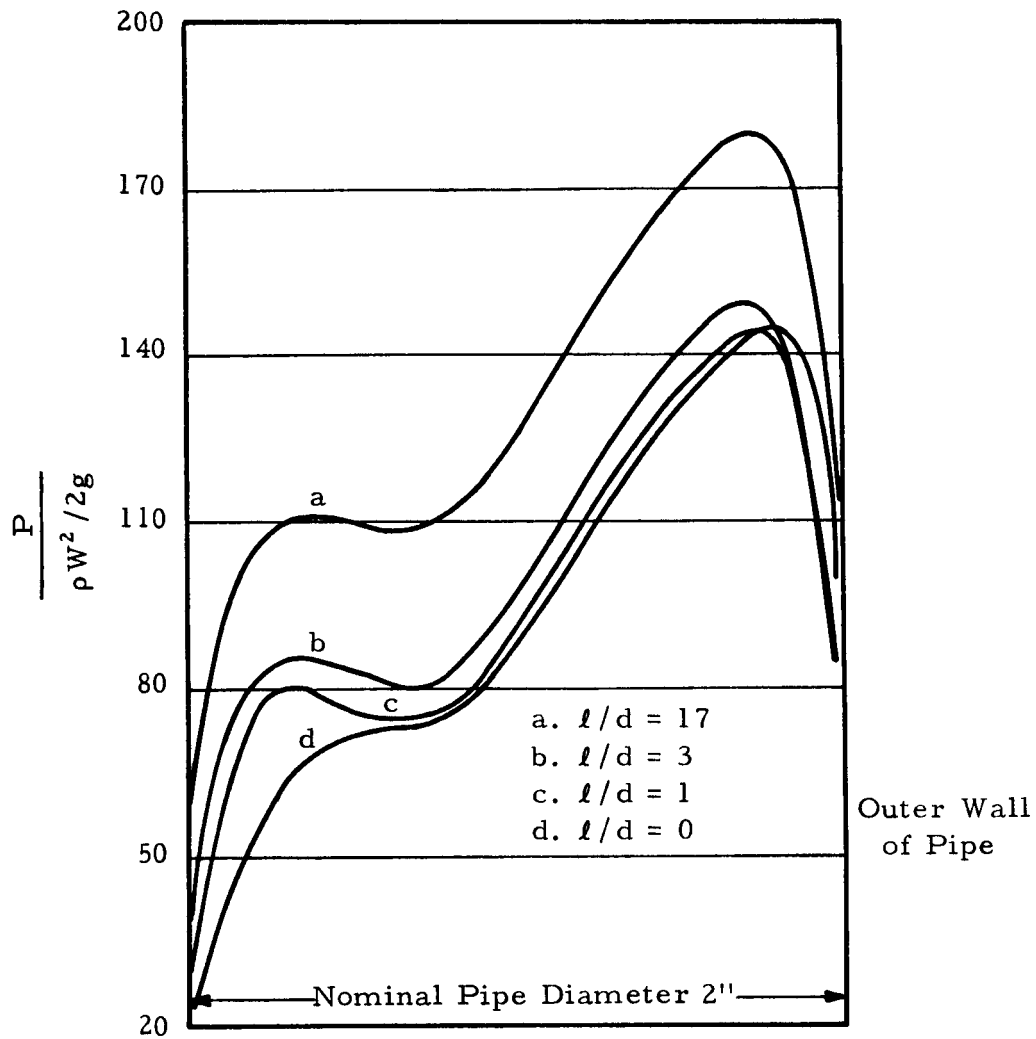
Figure 20. Variation of Total Pressure Profiles with Transition Length at the Outlet of a 70° Bend. Reynolds Number = 8.6×10^4.

$$\theta = k \, n \, \pi \left(\frac{2}{R/a}\right)^{\frac{1}{2}} \qquad n = 1, 2 \ldots \qquad . \tag{18}$$

The coefficient k is approximately equal to unity and must be experimentally determined and, among other things, will be a function of the velocity profile at the bend entrance and the length of the downstream tangent. If the bend is to be located proximate to the suction side of a turbo-pump, there is little to indicate that the presence of the pump, and especially one that induces pre-rotation in the suction pipe, will not significantly effect the experimental coefficient, k, and will perhaps even alter completely the flow process itself in the elbow including properties such as the minimum static pressure.

Since the flow mechanisms within an elbow are so sensitive to the presence of neighboring components, one must exercise caution in applying the results of investigations reported in the literature to a particular bend. Not until recently has this relationship been recognized and it quite possibly accounts for much of the lack of agreement between the results of the early investigations. Likewise, when planning any future experiments on flow in pipe bends, especially those that involve the sensitive inception of liquid cavitation, the conditions in the adjacent hardware must be carefully controlled before there can be any hope of obtaining reproducible results. For this reason, one is forced to add these external conditions to the already imposing array of variables affecting the flow in pipe bends.

The static pressure difference between the outside and the inside of a pipe bend has been found to be a simple and reliable method of measuring flow rates once the particular design has been calibrated under the appropriate conditions. This form of flow measurement is particularly useful since it can be located in an existing installation without introducing additional head loss from the measurement of the flow. Since the problem of predicting the absolute pressures in an elbow for a given flow rate is, in some respects, the inverse of the flow measurement application, some studies related to that problem will be briefly reviewed.

43

Under the conditions of inviscid free vortex flow, Addison[8] derived the following expression for the pressure difference across a bend of circular cross section in terms of the flow rate and bend geometry

$$P_o - P_i = \frac{1}{2g\rho} \left\{ \frac{\dot{m}}{C_d A} \frac{\left(\frac{R}{a}\right)^{\frac{1}{2}}}{\left[\left(\frac{R}{a}\right)^2 - 1\right]\left[\frac{R}{a} - \left(\frac{R}{a} - 1\right)^{\frac{1}{2}}\right]} \right\}^2 \tag{19}$$

where

P_o - the static pressure on the outside wall

P_i - the static pressure on the inside wall

a - the duct radius

C_d - a customary coefficient of discharge which must be experimentally determined to account for the nonideal flow.

Addison measured C_d at a point midway through a number of 4 inch diameter bends of various deflection angles and values of curvature ratio, R/a. The results are illustrated in Table 1. For the bends studied, the discharge coefficient was practically independent of average velocity at values of W greater than about 6.55 ft/sec.

Table 1 was taken under conditions of fully developed pipe flow at the entrance to the bend. As pointed out in the previous discussions, the nature of the flow within a pipe bend is strongly influenced by the proximate components, hence, the discharge coefficient must be a function of the conditions under which it was measured. In order to examine this influence, Addison also measured the discharge coefficients at a deflection angle of 45° in a number of 90° bends located within a permanent hydraulic installation and, except for two cases, found a surprisingly mild effect on C_d in both magnitude and variation with curvature ratio when compared with the tests under controlled conditions. However, the variation of C_d with

Table 1. Coefficients of Discharge for 4-Inch
Diameter Circular Bends (Reference 8)

Angle of Bend (degrees)	$\frac{R}{a}$	C_d
45	2.05	1.335
	4.00	1.081
	6.07	1.040
90	1.99	1.265
	4.11	1.050
	6.13	1.018
135	2.04	1.215
	4.11	1.075
	6.13	1.034

velocity was not as uniform as for those elbows tested under controlled conditions. This small effect on C_d might possibly indicate that the asymmetric entrance velocity profiles studied in References 4 and 5 were rather extreme situations obtained under laboratory conditions and not likely to be encountered in actual practice.

Complications arise when applying the knowledge of elbow flow meters to the problem of cavitation since it is now necessary to determine the absolute values for the pressure levels; not merely the pressure difference between the inner and outer walls. Furthermore, it is neces- sary that the static pressures, and any subsequently measured empirical parameters such as C_d, be referred to the deflection angle at which minimum pressure occurs at the inner wall. With these factors in mind, McPherson and Strausser[9] conducted a survey of existing experimental data and formulated an approximate potential analysis for predicting the minimum pressure at the inside wall of a duct bend which agreed fairly well with experimental data in the limited number of examples illustrated.

Unfortunately the analysis and comments were in reference to conduits of rectangular cross sectional shapes only and, hence, are inapplicable to the present study of ducts of circular cross section. Since the method appears to offer promise as a simple engineering approximation for determining minimum pressures in conduit bends, it will be derived herein for the case of circular cross sectional bends.

It is assumed that the flow approximates free vortex flow. Hence from Equation 15,

$$w'_i \, r_i = w' \, r = w'_o \, r_o = K \tag{20}$$

where the symbols have been previously defined.

Now the weight flow rate through the bend for a circular cross section is[8]

$$\dot{m} = 2\pi \, C_d \, K \, \rho \, c \left\{ \frac{R}{a} - \left[\left(\frac{R}{a} \right)^2 - 1 \right]^{\frac{1}{2}} \right\} . \tag{21}$$

Therefore from Equation 2

$$K = \frac{W \, a}{2 \, C_d \left\{ \frac{R}{a} - \left[\left(\frac{R}{a} \right)^2 - 1 \right]^{\frac{1}{2}} \right\}} . \tag{22}$$

For potential flow, the total pressure is always a constant throughout the flow field, therefore from Equation 14

$$p_i + \frac{\rho \, w'_i{}^2}{2g} = p_o + \frac{\rho \, w'_o{}^2}{2g} = p_m + \frac{\rho \, W^2}{2g} . \tag{23}$$

Hence the pressure at the inside wall in the plane of curvature is

$$p_i = p_m + \frac{\rho}{2g} (W^2 - w'_i{}^2) \tag{24}$$

which, with Equation 20, becomes

$$p_i = p_m + \frac{\rho}{2g} \left[W^2 - \left(\frac{K}{R - c} \right)^2 \right] . \tag{25}$$

46

Since the pressure at the inside wall is the minimum pressure in the bend for potential flow, the minimum pressure coefficient (Equation 4) becomes

$$C_{p_{min}} = \frac{p_1 - p_m - \frac{\rho}{2g}\left[W^2 - \left(\frac{K}{R-a}\right)^2\right]}{\frac{\rho W^2}{2g}} \qquad . \qquad (26)$$

The determination of the minimum pressure coefficient for a pipe bend for which the discharge coefficient is known now becomes a matter of determining the mean pressure, p_m, which is defined to be the static pressure in the plane of the bend at which the tangential velocity, w', is equal to the mean velocity, W. McPherson and Strausser suggest an approximate method of determining p_m but in the examples they presented, p_m is not too different from the static pressure at the bend inlet, p_1. Therefore, without introducing any errors greater than those already incurred by previous assumptions, let

$$p_m \simeq p_1 \qquad\qquad (27)$$

to a first approximation. The minimum pressure coefficient now becomes, with the aid of Equation 22,

$$C_{p_{min}} \simeq \left[2\,C_d\left\{\frac{R}{a} - \left[\left(\frac{R}{a}\right)^2 - 1\right]^{\frac{1}{2}}\right\}\left(\frac{R}{a} - 1\right)\right]^{-2} - 1 \qquad (28)$$

which is a function of bend geometry only since C_d is approximately independent of velocity except for extreme flow conditions such as separation, etc.

In order to illustrate the capabilities of the approximate analysis, a sample calculation will be compared with experimental data. Yarnell and Nagler[4] measured the pressures in a pipe bend under the following conditions:

$$a = 0.25 \text{ ft}$$

$$R = 0.688 \text{ ft}$$

$$W = 12.5 \text{ ft/sec}$$

$$p_1 = 355 \text{ lbf/ft}$$

Now

$$\frac{R}{a} = 2.75 \quad .$$

From Table 1, let

$$C_d = 1.1 \quad .$$

Now from Equation 22

$$K = \frac{(12.5)\,(0.25)\,(0.5)}{1.1\,\{2.75 - [(2.75)^2 - 1]^{\frac{1}{2}}\}}$$

$$K = 7.476 \text{ ft}^2/\text{sec} \quad .$$

From Equations 25 and 27, the pressure at the inside wall of the duct is

$$p_i = 355 + \frac{62.4}{64.4}\left[(12.5)^2 - \left(\frac{7.476}{0.688 - 0.25}\right)^2\right]$$

$$p_i = 224 \text{ lbf/ft}^2 \quad .$$

The measured minimum pressure occurred at a deflection angle of about 22.5° in the 90° bend and was approximately

$$p_i = 162 \text{ lbf/ft}^2 \quad ;$$

a difference of about 37% between the experimental and calculated values. The pressure at the outside wall may be found in a manner similar to Equation 25 for the inside pressure. Hence at the outside wall

$$p_o = p_m + \frac{\rho}{2g}\left[W^2 - \left(\frac{K}{R+a}\right)^2\right] \quad . \tag{29}$$

48

The computed pressure at the outside wall is then

$$p_o = 445 \ \text{lbf/ft}^2$$

and the measured value was approximately

$$p_o = 422 \ \text{lbf/ft}^2 \ .$$

The nature of the discrepancy between the calculated and measured inside and outside pressures suggests that the mean pressure is actually lower rather than equal to the inlet pressure. In order to examine this possibility, a value of C_d was computed from the pressure difference measured at a deflection angle of 22.5° and was found to be

$$C_d = 1.0305$$

which is less than the value assumed for the comparison. The pressures at the inner and outer walls were computed once again using this value of C_d and the computed values still exceeded the experimental values indicating that the entrance pressure, p_1, was greater than the mean pressure, p_m, by about 22 lbf/ft^3 thus illustrating the validity of Equation 27 within about 10% at least for the case considered. This example also illustrates the strong influence that the assumed value of C_d has upon the results because of its being squared when solving for the pressures.

The velocities in the major portion of the fluid have been observed to qualitatively conform to that described by ideal flow potential theory (Equation 20). The pressures corresponding to ideal flow ($C_d = 1$) were computed from Equation 24 and found to be, assuming $p_m = 333 \ \text{lbm/ft}^3$,

$$p_i = 132 \ \text{lbf/ft}^2$$

$$p_o = 410 \ \text{lbf/ft}^2$$

hence, by comparison with the measured pressures, the flow also closely conforms quantitatively to that predicted by the ideal inviscid flow theory.

49

The exception is at the inside wall where there is a jump in static pressure resulting from the two secondary currents at the wall rotating to the inside and impinging at the plane of symmetry. Since the ideal theory does not include any viscous effects, it should be expected to predict pressures at the inside wall lower than those actually encountered. Furthermore, since the point of minimum pressure in the pipe is not located immediately adjacent to the inner wall but some distance towards the duct centerline, the ideal value of minimum pressure, which governs the onset of cavitation, will be closer to the actual minimum pressure than that measured by a static pressure tap at the inside wall. This pressure jump at the inside wall has unfortunate implications from the standpoint of experimentally investigating the cavitation characteristics (minimum pressure) of elbow flow since now all references to the physical location of the point of minimum static pressure must not be referred to the inside wall but to some point within the flow where static pressure measurements are difficult to obtain accurately because of the three dimensional nature of the flow.

To more clearly illustrate the relationship between the minimum pressure coefficient and the bend geometry, Equation 28 was evaluated for various values of R/a and C_d and presented in Figure 21. For cavitation considerations, the consequences of selecting a curvature ratio less than about 3 are obvious since the minimum pressure coefficient begins to drastically increase (minimum pressure decreases) with any lower values. Although the data of Addison, which was presented primarily for illustration purposes, indicated for the most part an independence of C_d, and hence $C_{p_{min}}$, on velocity, this will not be the case at higher velocities (and lower values of R/a) since flow separation at the inside wall will be induced and will significantly alter the flow processes. For this reason and others elaborated on earlier, more information must be obtained on the assumption of Equation 27 and values of C_d must be calculated from more exact analyses or preferably generated experimentally under conditions approximating the actual situations before this semiempirical technique can be usefully employed for design purposes.
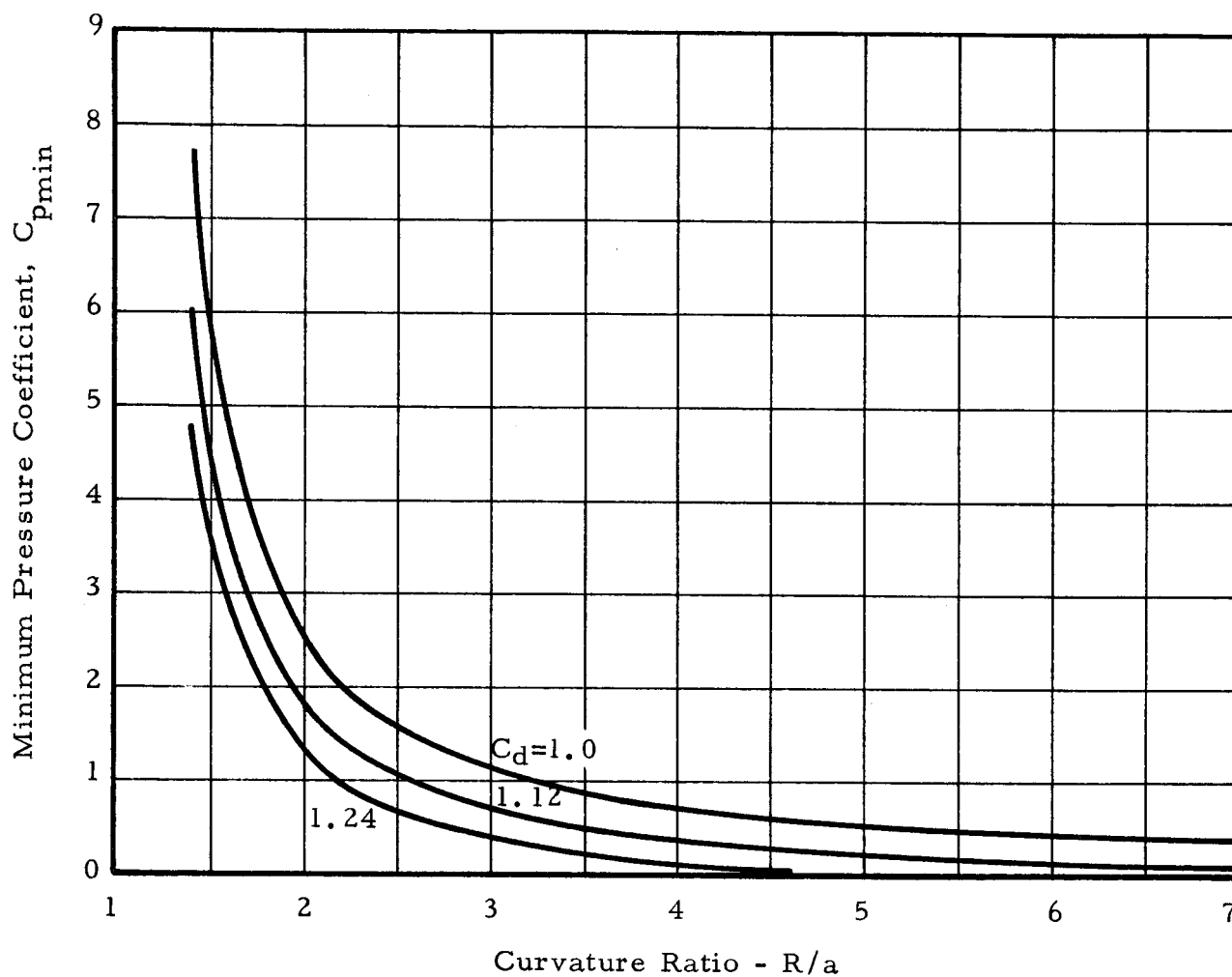
50

Figure 21. Minimum Pressure Coefficient as a Function of
Curvature Ratio and Discharge Coefficient -
Potential Solution

51

Before proceeding further, a sample problem will be calculated for a specific design situation in order to illustrate application of the theory. Assume that liquid nitrogen with a vapor head of 44.2 feet flows through a 90° pipe bend at an average velocity of 50 ft/sec. The cavitation inception occurs as a known function of velocity (Figure 6, Reference 10). Thus,

$$\sigma_i = f(W) \, C_{P_{min}}$$

and the discharge coefficient is assumed to be unity (ideal potential flow).

Now from the definition of the inception cavitation parameter, σ_i (in terms of head rather than pressure) we can compute the static head at the entrance to the elbow at which cavitation will first become apparent in the bend itself. That is, for inception of cavitation,

$$h_{1i} = \frac{W^2}{2g} \, \sigma_i + h_V \quad . \tag{30}$$

Figures 22 and 23 illustrate the resultant variation of static head with the bend curvature and average velocity. Here again, one is reminded of the necessity of maintaining as large a bend curvature and low a velocity as is possible in order to achieve an optimum system design from the cavitation standpoint since small curvatures and high velocities require higher inlet static heads and therefore a higher initial total head for a given upstream ducting system with its associated losses.

In summarizing the discussion of the experimental investigations, the flow in an elbow of circular cross section and constant radius of curvature may be divided into three separate but interrelated regions. The "shedding layer" is composed of a layer of fluid near the walls which has been retarded by viscosity and which has a peripheral velocity component towards the inside of the pipe bend in addition to the primary axial velocity component. The "core" of the fluid which is outside the shedding layer and unaffected by viscosity is essentially governed by potential flow

$$W = 50 \text{ ft/sec}$$
$$\sigma_i = 0.66 \, C_{p_{min}}$$
$$C_d = 1.0$$

No Cavitation

Cavitation

h_v

h_{l_i} - ft

R/a
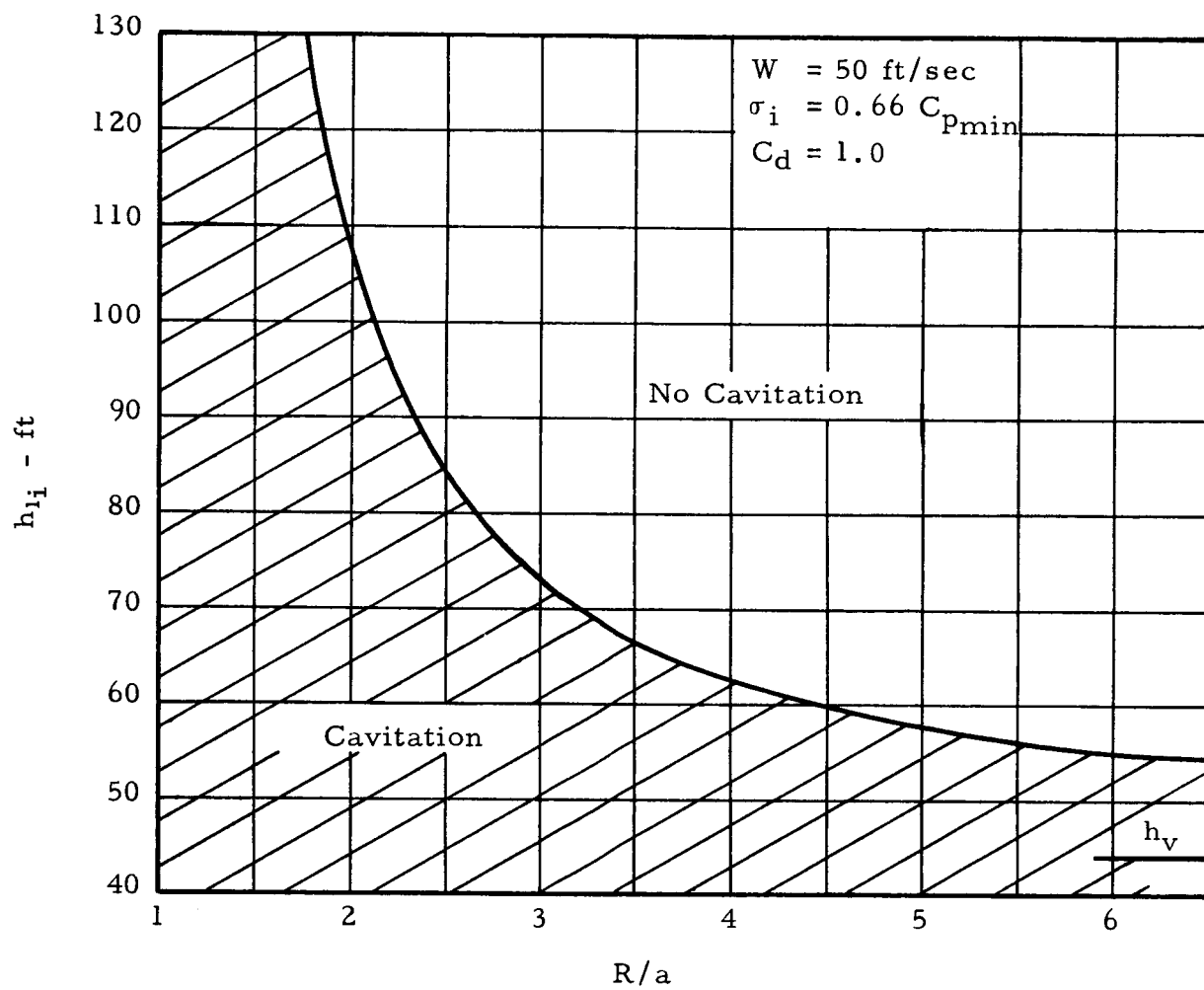
Figure 22. Static Head at the Entrance to a 90° Bend at Which
Cavitation Will Occur in Liquid Nitrogen
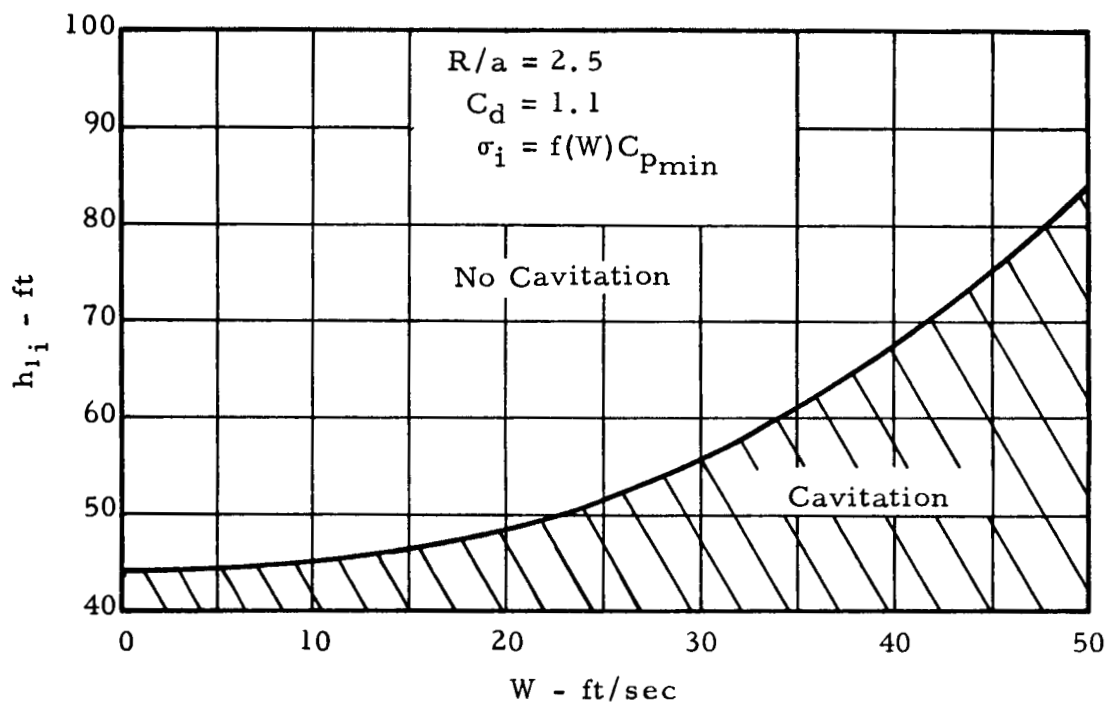
Figure 23. Static Pressure Head at the Entrance to a 90° Bend
at which Cavitation Will Not Occur in Liquid Nitrogen

54

considerations, at least in the transition part of a curved pipe for the limited conditions examined. The "region of eddy flow" exists at the inside wall of the bend where the opposing shear layers impinge and form a region of nearly stagnant, low energy fluid.

The combination of shedding layer flow and the core flow form a system of double vortices, one above and one below the plane of curvature, which are oscillatory in the region of transition from the entering recti-linear flow to fully developed curved pipe flow. These vortices which are strongly influenced by the entrance and exit flow conditions, persist far into the downstream pipe depending upon the strength of the vortex at the bend outlet. A simple potential vortex solution indicated that the minimum pressure, which is of primary consideration from the standpoint of cavitation inception, decreases quite rapidly with values of the curvature ratio, R/a, less than about three.

REVIEW OF ANALYTICAL CURVED FLOW RESEARCH

The reported analytical treatments of curved pipe flow are even fewer in number than experimental investigations, and because of the numerous simplifying assumptions of one form or another, they generally fail to yield any new information on the basic flow fundamentals pertaining to the present problem. As far as could be determined, all analytical treatments of viscous curved pipe flow are restricted to fully developed flow, e.g., flow that occurs in a helical coil a sufficient distance from the inlet so that equilibrium has been established between the various viscous and dynamical influences that cause the initial oscillations in performing the transition from rectilinear to curvilinear motion. The fully developed flow is more amenable to analysis than the transition type of flow that occurs in a finite elbow and at the entrance and exits of a coiled pipe because the velocity profiles are similar at different stations and hence all derivatives in the stream direction are either constant or dissappear entirely. A number of other analyses are applicable only to curved channels of large depth, thus simplifying the problem considerably since there will be no viscosity generated secondary currents such as occur in curved pipes with closed cross sectional shapes. Nevertheless, in spite of the limitations, a few of the more prominent curved pipe solutions will be reviewed in the expectation that some contribution might be of value for future analytical undertakings.

In general, the reported solutions to curved pipe flow may be divided into two classifications as follows:

1. Solution to the hydrodynamic equations.

2. Shedding layer solutions.

The common parameter to be used for the evaluation of these solutions will be the minimum pressure coefficient. The general assumption will be made that the pressure at the centerline is equal to the uniform reference

static pressure, p_1. In order to avoid repetition, the various treatments will be discussed collectively within their particular classifications.

Solutions to the Hydrodynamic Equations

The hydrodynamic equations governing the flow of an incompressible, Newtonian fluid in the torodial coordinate system illustrated in Figure 24 are:

The Navier Stokes Equations:

$$u \frac{\partial u}{\partial r} + \frac{v}{r} \frac{\partial u}{\partial \psi} + \frac{w}{R + r \sin \psi} \frac{\partial u}{\partial \theta} - \frac{v^2}{r} - \frac{\sin \psi}{R + r \sin \psi} w^2 = -\frac{1}{\rho} \frac{\partial p}{\partial r} + \nu \left\{ \frac{\partial^2 u}{\partial r^2} + \frac{1}{r^2} \frac{\partial^2 u}{\partial \psi^2} \right.$$

$$+ \frac{1}{(R + r \sin \psi)^2} \frac{\partial^2 u}{\partial \theta^2} + \frac{(R + 2r \sin \psi)}{r(R + r \sin \psi)} \frac{\partial u}{\partial r} + \frac{\cos \psi}{r(R + r \sin \psi)} \frac{\partial u}{\partial \psi} - \frac{2}{r^2} \frac{\partial v}{\partial \psi}$$

$$- \frac{2 \sin \psi}{(R + r \sin \psi)^2} \frac{\partial w}{\partial \theta} - \left[\frac{1}{r^2} + \frac{\sin^2 \psi}{(R + r \sin \psi)^2} \right] u - \cos \psi \frac{(R + 2r \sin \psi)}{r(R + r \sin \psi)^2} v \left. \right\}$$

$$(31a)$$

$$u \frac{\partial v}{\partial r} + \frac{v}{r} \frac{\partial v}{\partial \psi} + \frac{w}{R + r \sin \psi} \frac{\partial v}{\partial \theta} + \frac{uv}{r} - \frac{\cos \psi}{R + r \sin \psi} w^2 = -\frac{1}{\rho r} \frac{\partial p}{\partial \psi} + \nu \left\{ \frac{\partial^2 v}{\partial r^2} + \frac{1}{r^2} \frac{\partial^2 v}{\partial \psi^2} \right.$$

$$+ \frac{1}{(R + r \sin \psi)^2} \frac{\partial^2 v}{\partial \theta^2} + \frac{R + 2r \sin \psi}{r(R + r \sin \psi)} \frac{\partial v}{\partial r} + \frac{\cos \psi}{r(R + r \sin \psi)} \frac{\partial v}{\partial \psi} - \frac{2 \cos \psi}{(R + r \sin \psi)^2} \frac{\partial w}{\partial \theta}$$

$$+ \frac{2}{r^2} \frac{\partial u}{\partial \psi} + \frac{R \cos \psi}{(R + r \sin \psi)^2} \frac{u}{r} - \left[\frac{r(r + R \sin \psi) + R(R + r \sin \psi)}{r^2 (R + r \sin \psi)^2} \right] v \left. \right\}$$
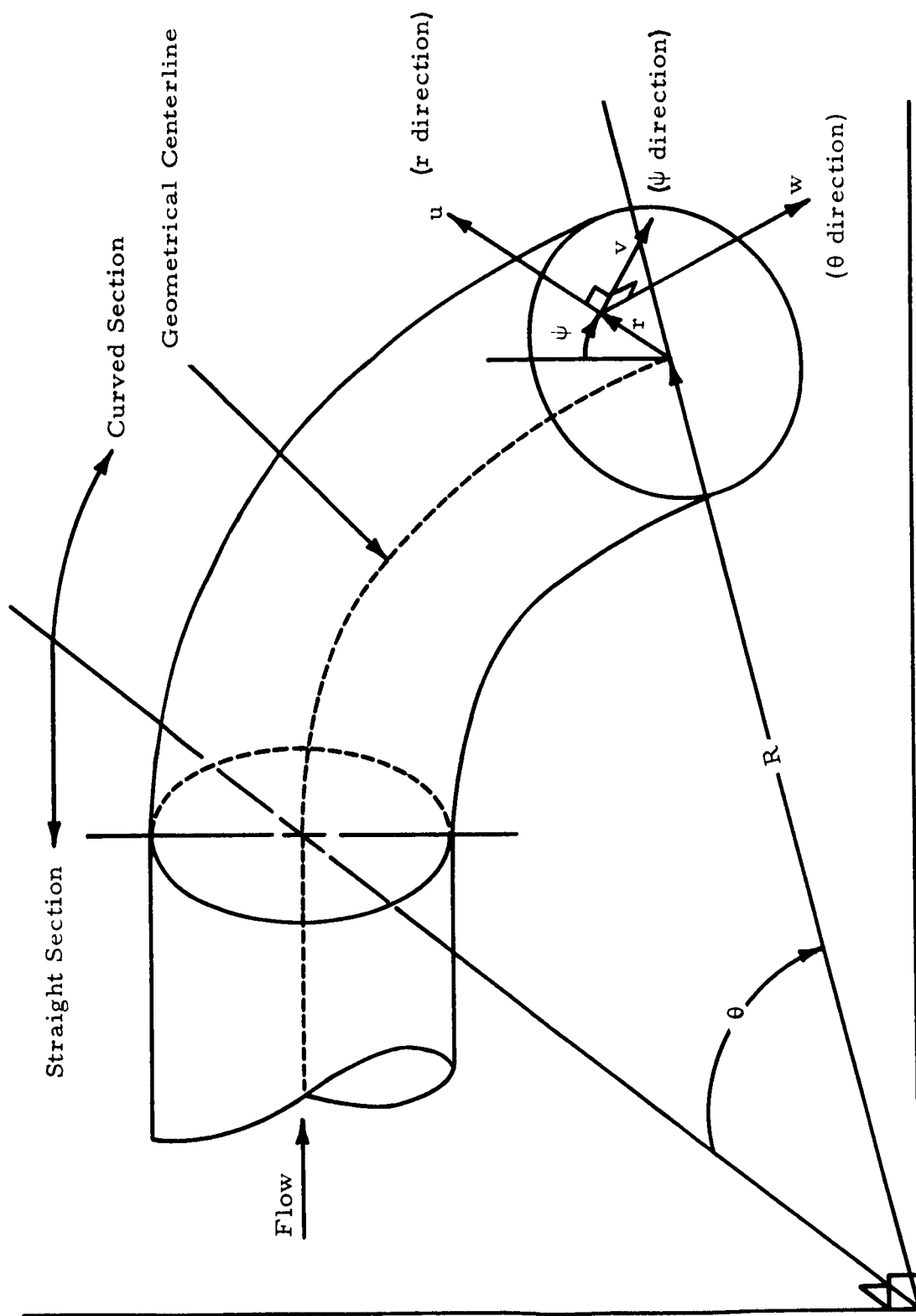
$$(31b)$$

57

Figure 24. Torodial Coordinate System (r, ψ, θ)

Curved Section

Geometrical Centerline

u (r direction)

(ψ direction)

w

(θ direction)

v

ψ

r

Straight Section

R

θ

Flow

58

$$u\frac{\partial w}{\partial r} + \frac{v}{r}\frac{\partial w}{\partial \psi} + \frac{w}{R+r\sin\psi}\frac{\partial w}{\partial \theta} + \frac{\cos\psi}{R+r\sin\psi}vw + \frac{\sin\psi}{R+r\sin\psi}uw =$$

$$-\frac{1}{(R+r\sin\psi)\rho}\frac{\partial p}{\partial \theta} + \nu\left[\frac{\partial^2 w}{\partial r^2} + \frac{1}{r^2}\frac{\partial^2 w}{\partial \psi^2} + \frac{1}{(R+r\sin\psi)^2}\frac{\partial^2 w}{\partial \theta^2} + \frac{(R+2r\sin\psi)}{r(R+r\sin\psi)}\frac{\partial w}{\partial r}\right.$$

$$\left. + \frac{\cos\psi}{r(R+r\sin\psi)}\frac{\partial w}{\partial \psi} + \frac{2\sin\psi}{(R+r\sin\psi)^2}\frac{\partial u}{\partial \theta} - \frac{2\cos\psi}{(R+r\sin\psi)^2}\frac{\partial v}{\partial \theta} - \frac{w}{(R+r\sin\psi)^2}\right]$$

$$(31c)$$

Continuity Equation:

$$\frac{\partial u}{\partial r} + \frac{1}{r}\frac{\partial v}{\partial \psi} + \frac{1}{R+r\sin\psi}\frac{\partial w}{\partial \theta} + \frac{R+2r\sin\psi}{r(R+r\sin\psi)}u + \frac{\cos\psi}{R+r\sin\psi}v = 0 \qquad (31d)$$

where u, v, and w are the velocity components in the r, ψ, θ, directions respectively.

Dean[11] first obtained a solution to this complicated set of equations by assuming fully developed coiled pipe flow and the ratio, R/a, is very large. These assumptions enabled him to neglect all derivatives of velocity with respect to θ and to simplify other terms containing R + r sin ψ. The resulting solution was obtained as a small perturbation from straight pipe laminar flow and, therefore, is not applicable to high velocity or to small radius of curvature; specifically it is valid for small values of Dean's number, D, only.

Dean presented the relations for the velocity components from which it is possible to easily determine the minimum pressure coefficient

$$C_{p_{min}} = \frac{\frac{5}{3}}{\frac{R}{a}} \qquad . \qquad (32)$$

Comparison with the free vortex solution presented in Figure 20 gives good agreement for values of R/a greater than about 6 or 7. Clearly, the Dean analysis (Equation 32) is not adequate for the present application where smaller values of the R/a ratio are encountered.

Although Dean's analysis included the effects of friction, one notes that the pressure coefficient contains no terms involving viscosity. This is due to the low order of approximation of that analysis. In a subsequent publication[12] Dean included higher order terms in a series expansion of D^2. Although he only presents results up through the second approximation by which the pressure coefficient may be obtained (with some labor), he carried out the successive approximation process to the fourth term and reports that the results are probably not valid for values of D^2 greater than 400 which is still too low for the present application to high flow rates and small radius of curvature. For this reason we will make no attempt to obtain the minimum pressure coefficient for the second approximation of Dean.

Cuming[13] and Ito[14] extended the successive approximation technique of Dean to include elliptical and square flow cross sections in curved pipes. Since the restrictive assumptions for these analyses are the same as for Dean's regarding their applicability to pipe bends of small radius of curvature and large flow rates, the labor involved to obtain the pressure coefficient does not make a comparison worthwhile for the present applications. However, it is interesting to examine the effect of cross sectional shape on the flow as compared with pipes of circular cross section.

The intensity of the secondary circulation[13] in an elliptical cross section is a maximum, about three times that for a circular pipe, when the ratio of the ellipse axis normal to the plane of curvature to the axis in the plane of curvature (λ) is about 2. When $\lambda > 6$ and $\lambda < 1$, the intensity of secondary circulation becomes less than for a pipe of circular cross sectional shape. If this situation maintains itself for small radius of

60

curvature and high flow rates, then apparently one method of reducing the intensity of the secondary circulation in the downstream tangent of a pipe elbow is to employ an elliptical cross sectional shape in the bend with the major axis in the plane of curvature and the minor axis normal to it. Such a possibility is worth exploring in an investigation of techniques for minimizing flow distortion resulting from flow turning.

Shedding Layer Solution

The possibility of obtaining solutions for the large Reynolds numbers in the laminar and turbulent flow regimes appears to exist in the shedding layer concept. This technique was first applied by Adler[15] and later by Barua[16, 17] to laminar flow and extended by Ito[18] to turbulent flow. Weske[19] employed the shedding layer concept in an analysis of loss coefficients in curved pipes but, on brief examination, the results do not appear applicable to the present problem of determining the static pressure profiles.

The technique, which thus far has been used only for the case of fully developed curvilinear flow, consists of solving the following governing equations in a modified rectangular coordinate system (Figure 25).

The Navier Stokes Equations:

$$u' \frac{\partial u'}{\partial x} + v' \frac{\partial u'}{\partial y} + \frac{w'}{R+x} \frac{\partial u'}{\partial \theta} - \frac{w'^2}{R+x} = -\frac{\partial}{\partial x}\left(\frac{p}{\rho}\right) + \nu \left[\frac{\partial^2 u'}{\partial x^2} + \frac{1}{R+x} \frac{\partial u'}{\partial x} \right.$$

$$\left. + \frac{\partial^2 u'}{\partial y^2} + \frac{1}{(R+x)^2} \frac{\partial^2 u'}{\partial \theta^2} - \frac{2}{(R+x)^2} \frac{\partial w'}{\partial \theta} - \frac{u'}{(R+x)^2} \right] \tag{32a}$$

$$u' \frac{\partial v'}{\partial x} + v' \frac{\partial v'}{\partial y} + \frac{w'}{R+x} \frac{\partial v'}{\partial \theta} = -\frac{\partial}{\partial y}\left(\frac{p}{\rho}\right) + \nu \left[\frac{\partial^2 v'}{\partial x^2} + \frac{1}{R+x} \frac{\partial v'}{\partial x} \right.$$

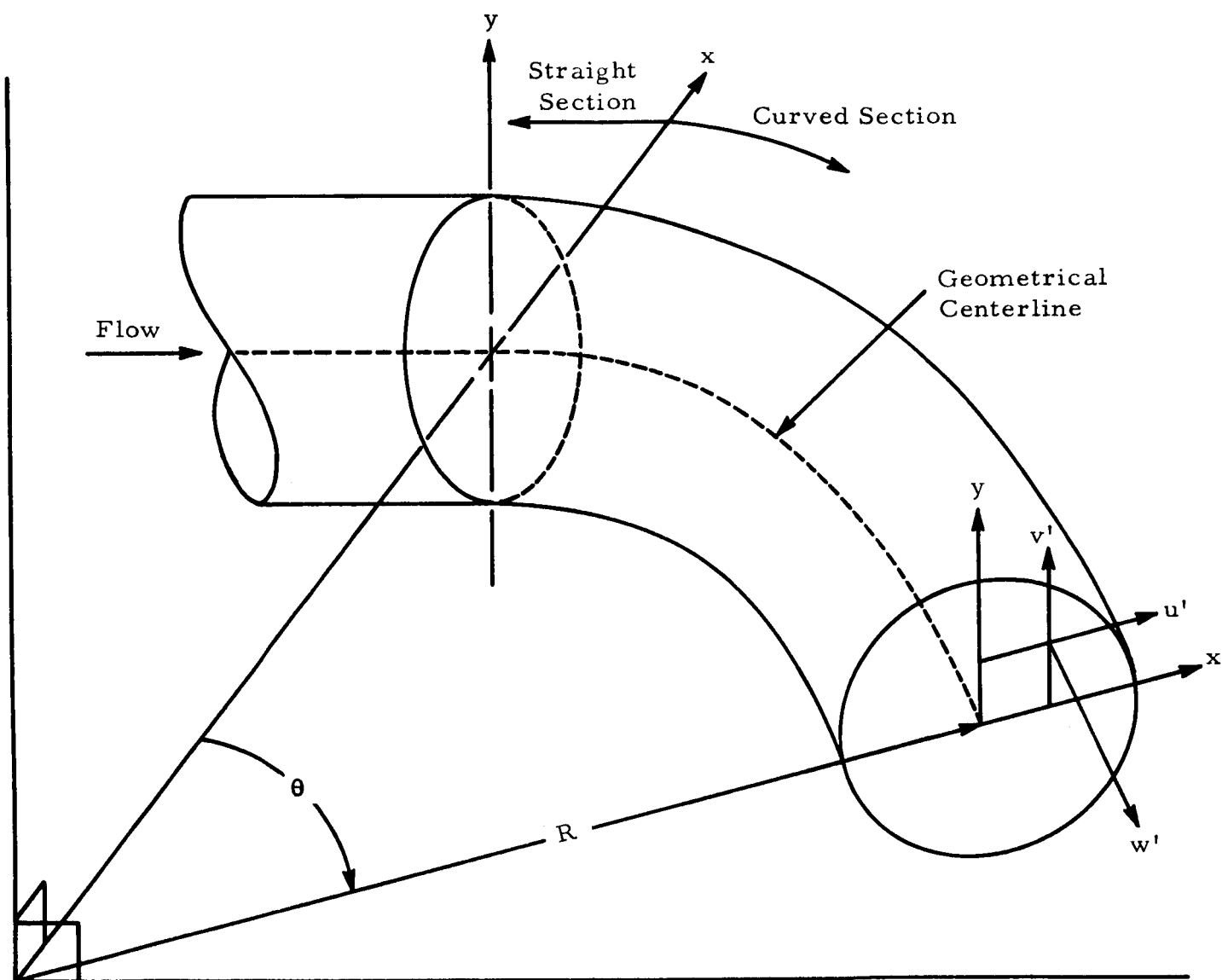$$\left. + \frac{\partial^2 v'}{\partial y^2} + \frac{1}{(R+x)^2} \frac{\partial^2 v'}{\partial \theta^2} \right] \tag{32b}$$

61

Figure 25. Modified Rectangular Coordinate System (x, y, θ)

$$u' \frac{\partial w'}{\partial x} + v' \frac{\partial w'}{\partial y} + \frac{w'}{R+x} \frac{\partial w'}{\partial \theta} + \frac{u'w'}{R+x} = -\frac{1}{R+x} \frac{\partial}{\partial \theta}\left(\frac{p}{\rho}\right) + \nu \left[\frac{\partial^2 w'}{\partial x^2} \right.$$

$$\left. + \frac{1}{R+x} \frac{\partial w'}{\partial x} + \frac{\partial^2 w'}{\partial y^2} + \frac{1}{(R+x)^2} \frac{\partial^2 w'}{\partial \theta^2} + \frac{2}{(R+x)^2} \frac{\partial u'}{\partial \theta} - \frac{w'}{(R+x)^2} \right]$$

(32c)

Continuity Equation:

$$\frac{\partial u'}{\partial x} + \frac{\partial v'}{\partial y} + \frac{1}{R+x} \frac{\partial w'}{\partial \theta} + \frac{u'}{R+x} = 0 \quad .$$

(32d)

The inviscid core flow is first analyzed by assuming a functional relationship for one of the velocity components. Barua assumed that the v' component of velocity is zero, Figure 26. Integrating the continuity equation (remembering that θ derivatives are zero) gives

$$u' = \frac{A}{R+x} \quad .$$

(33)

By assuming a constant pressure gradient in the θ direction (compatible with fully developed flow) the θ component of the momentum equation may be directly integrated to give the axial or tangential component of velocity

$$w' = \frac{B}{2A}\left(R + x + \frac{C}{R+x}\right)$$

(34)

where the constants A, B, and C must be determined. This velocity variation is observed to differ from the free vortex solution by the term

$$\frac{B}{2A}(R+x) \quad .$$

The x component of the momentum (Equation 32a) may now be integrated to give the pressure variation in the pipe cross section for inviscid flow

$$\frac{p}{\rho} = \frac{B^2}{4A^2}\left[\frac{(R+x)^2}{2} + 2C \ln (R+x) - \left(\frac{C^2}{2} + \frac{2A^4}{B^2}\right)\frac{1}{(R+x)^2}\right] - B\theta + \text{constant} \quad .$$
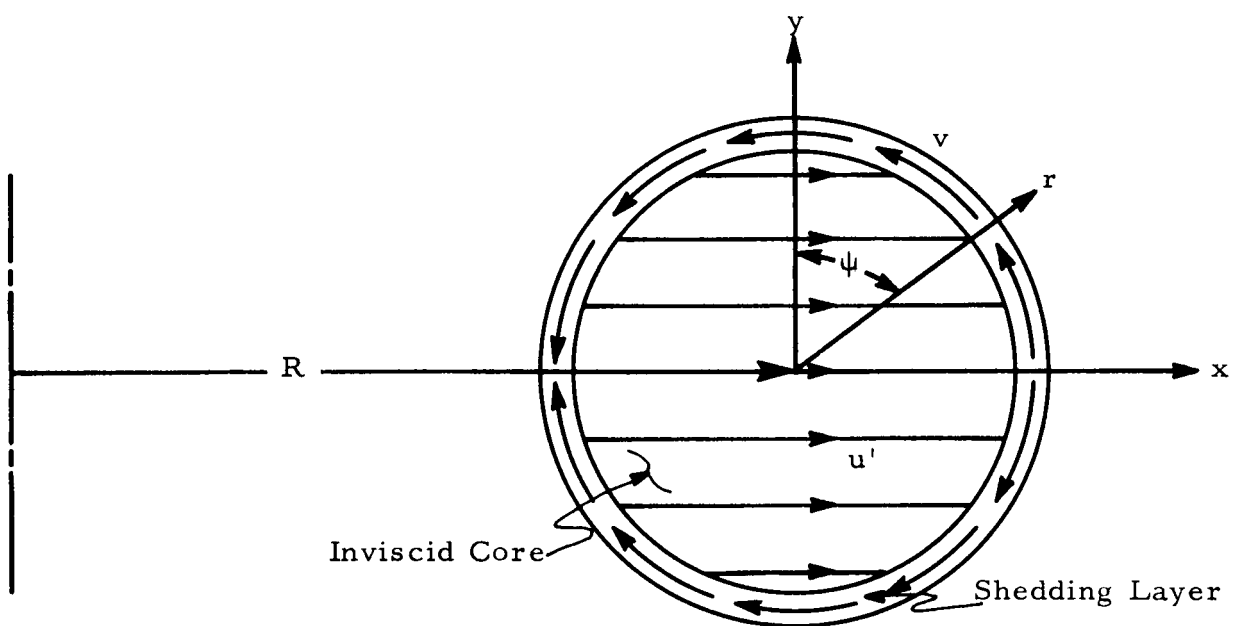
(35)

Figure 26. Shedding Layer Model for Fully Developed
Curvilinear Flow

It is always necessary that mass be conserved hence the transport of mass to the outside of the pipe by the u' component of velocity in the inviscid core flow must be balanced by a flow of mass to the inside of the pipe through the shedding layer. A solution of the shedding layer will therefore be based upon the mass balance requirement and will yield the constants A, B, and C resulting in a coupling between the inviscid core flow and the viscous shedding layer flow.

The flow in the shedding layer is governed by the continuity and Navier Stokes equation in the torodial coordinate system, and the thickness is assumed to be thin with respect to the pipe radius, a, so that the boundary layer concept is applicable. The Von Karman-Pohlhausen integral method which requires an assumed function for the velocity profiles in the shedding layer is employed to solve the resultant equations. Barua employed simple power series expressions for the axial and peripheral velocity components w and v which satisfy the requirements that the derivatives with r disappear at the edge of the shedding layer and the velocities themselves disappear at the walls. The following expressions for the constants may be obtained from Barua's theory:

$$\frac{C}{a^2} = C'$$

$$= -\left(\frac{R}{a}\right)^2 + \sqrt{6}\left(\frac{R}{a}\right)$$

(36)

$$\frac{B}{W^2} = B'$$

$$= \frac{5.635\left(\frac{R}{a}\right)^{3/2}}{R_e^2}\left\{1.181 + \left[1.395 + \frac{R_e}{2.45\left(\frac{R}{a}\right)^{\frac{1}{2}}}\right]^{\frac{1}{2}}\right\}^3$$

(37)

$$\frac{A}{\frac{\rho}{\mu}} = A'$$

$$= 1.259 \left(\frac{R}{a}\right)^{\frac{1}{2}} \left(\frac{R_e^2 \, B'}{4}\right)^{1/3} \quad .$$

The minimum pressure coefficient may now be obtained from Equation 35

$$C_{P_{min}} = \frac{R_e^2 \, B'^2}{8 A'^2} \left(\frac{1}{2} \left\{ \left(\frac{R}{a}\right)^2 - \left[\left(\frac{R}{a}\right)^2 - 1\right]^2 \right\} + 2\,C'\,\ell n \, \frac{\left(\frac{R}{a}\right)}{\left(\frac{R}{a}\right) - 1} \right.$$

$$\left. - \left(\frac{32\,A'^4}{R_e^4 \, B'^2} + \frac{C'^2}{2}\right) \left\{ \frac{1}{\left(\frac{R}{a}\right)^2} - \frac{1}{\left[\left(\frac{R}{a}\right) - 1\right]^2} \right\} \right)$$

where, as was previously stated, it is assumed that there is negligible contribution to the pressure coefficient due to the centerline pressure drop.

Equation 39 was evaluated for various values of curvature ratio, R/a, and presented in Figure 27 with Reynolds number as a parameter. Comparison is made with the free vortex potential solution (Equation 28) and the Dean first order solution (Equation 32). The three theories are observed to tend towards approximately a common result as the radius of curvature increases with perhaps the potential solution being slightly greater than the two viscous solutions. Also, the tendency for $C_{P_{min}}$ to decrease with increasing Reynolds number in accord with the results of the free vortex solution for increasing values of C_d (Figure 21).

Comparison of loss coefficient data with theory[16] indicates that the theory is most accurate for values of R/a less than about 6.0 for the Reynolds numbers considered in Figure 27. However, at values of R/a less than about 3.0, the Barua theory yields $C_{P_{min}}$ values greater than the potential solution. This may quite possibly be due to the fact that the
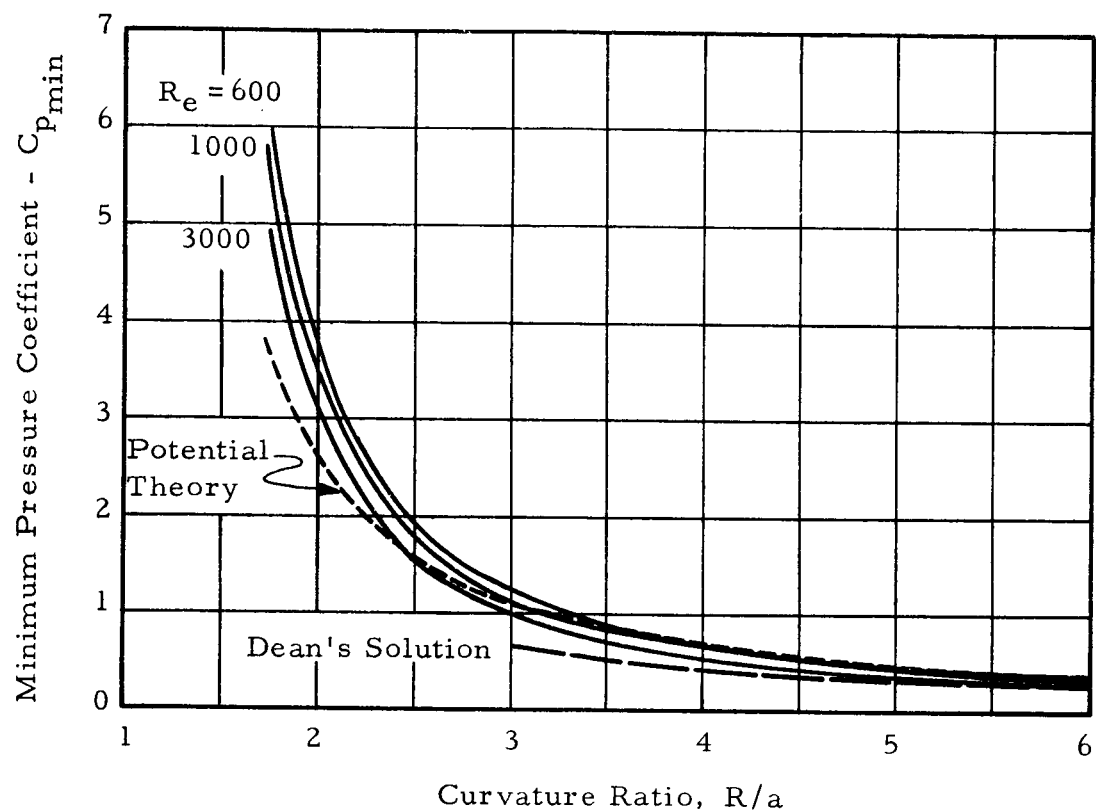
Figure 27. Minimum Pressure Coefficient as a Function of Curvature Ratio and Reynolds Number - Shedding Layer Solution (Barua)

particular shedding layer solution of Barua applies to fully developed pipe
flow where the secondary flow processes have had the opportunity to dis-
tort the potential flow which, as limited experimental data indicates, exists
in the entrance or transition region. Evaluation of the axial velocity com-
ponent w' from Equation 34 indicates that the Barua theory yields velocity
relationships which are far from potential and, hence, are not in accord
with the experimentally observed core velocities in the transition region
(elbows of approximately 90° deflection angle). One would intuitively
reason that the secondary flow processes which occur due to friction would
transport fluid of low momentum to the inner wall and thus by retarding
action, increase the pressure at the inner wall (decrease $C_{p_{min}}$) above
that resulting from the ideal free vortex case ($C_d = 1.0$). These arguments
and the results of Figure 27 indicate, therefore, that Barua's theory should
be conservative from the standpoint of application to cavitation tendency of
finite elbows where the core flow is known to approximate the potential
condition in the transition region.

The pressure coefficients for the two remaining shedding layer
solutions (Adler[15] and Ito[18]) were not derived in the present survey. They
both assumed an axial velocity profile of the form

$$w' = A + B (R + x)$$

which does not include a term proportional to $(R + x)^{-1}$ and hence is not
even approximately similar to potential profile which is existent in the
transition region of an elbow for entering turbulent flow. It would be of
interest to compare the turbulent theory of Ito[18] with the laminar theory
of Adler but unfortunately Ito did not present the solutions for A and B
and the reference in which he indicates they may be found[20] was not
available for the present survey.

CONCLUSIONS

The preceding discussions are primarily an attempt to illustrate the salient features of curved duct flow. Since there is a total absence of experiments related to the liquid cavitation phenomenon, the need for research in this area is obvious. In addition, there has been inadequate study of the static pressures attained in a pipe bend, especially under the conditions of the present application. The distortion of flow patterns incurred from turning the flow has been investigated to the extent that only certain qualitative generalizations may be made in regards to its persistence in the downstream tangent under realistic conditions at the bend entrance.

Insofar as could be determined, there are no analytical developments available which treat the transition type of flow that occurs in the entrance and exit regions of an elbow. Independent study indicates that certain mathematical difficulties exist which present formidable obstacles to be overcome in any analytical description of this type of flow. For this reason, experimentation will, in all likelihood, provide the bulk of the information on flow in pipe elbows for the near future.

In relation to the cavitation phenomenon in elbows, there were illustrated two analyses by which one may obtain the minimum pressure coefficient in fully developed coiled pipe flow under the assumptions of zero flow losses. In order to apply these techniques to the computation of the minimum pressure coefficient in an elbow, one must assume that part way through the bend fully developed flow is established. Since this is an unlikely possibility for the most useful bend deflection angles, one must again rely on experimental data to establish the accuracy of these analyses before they can be usefully employed for purposes of designing cavitation free pipe bends.

69

REFERENCES

1. Eustice, John, "Experiments on Streamline Motion in Curved Pipes", Proceedings of the Royal Society (London), Series A, Vol. 85, pp. 119-131 (1911)

2. Taylor, G. I., "The Criterion for Turbulence in Curved Pipes", Proceedings of the Royal Society (London), Series A, Vol. 124, pp. 243-249 (1929)

3. White, C. M., "Streamline Flow through Curved Pipes", Proceedings of the Royal Society (London), Series A, Vol. 123, pp. 645-659 (1929)

4. Yarnell, David L. and Floyd A. Nagler, "Flow of Water Around Bends in Pipes", American Society of Civil Engineers, Vol. 100, pp. 1018-1043 (1935)

5. Weske, John R., "Experimental Investigation of Velocity Distribution Downstream of Single Duct Bends", National Advisory Committee for Aeronautics, Technical Note No. 1471, January, 1948

6. Hawthorne, W. R., "Secondary Circulation in Fluid Flow", Proceedings of the Royal Society (London), Series A, Vol. 206, pp. 374-387 (1951)

7. Martin, Moira E. and E. C. Deverson, "The Effect of Bend Outlet Conditions on the Pressure Losses in Bent Circular Pipes", D.D.G. (Eng.), Ref: Eng. R280/0/21, TIL (BR) 266, 1957 (AD142886)

8. Addison, Herbert, "The Use of Pipe Bends as Flow Meters", Engineering, pp. 227-229, March 4, 1938

9. McPherson, M. B. and H. S. Strausser, "Minimum Pressures in Rectangular Bends", Proceedings of the American Society of Civil Engineers, Paper 747, Vol. 81, July, 1955

10. Ruggeri, Robert S. and Thomas F. Gelder, "Cavitation and Effective Liquid Tension of Nitrogen in a Tunnel Venturi", National Aeronautics and Space Administration, TN D-2088, February, 1964

11. Dean, W. R., "Note on the Motion of Fluid in a Curved Pipe", Philosophical Magazine, Series 7, Vol. 4, No. 20, pp. 208-223, July, 1927

12. Dean, W. R., "The Streamline Motion of Fluid in a Curved Pipe", Philosophical Magazine, Series 7, Vol. 5, No. 30, pp. 673-695, April, 1928

13. Cuming, H. G., "Secondary Flow in Curved Pipes", Aeronautical Research Council, R & M No. 2880, 1955 (AD104933)

14. Ito, Hidesato, "Theory on Laminar Flows Through Curved Pipes of Elliptic and Rectangular Cross Sections", Reports of the Institute of High Speed Mechanics, Tohoku University, Vol. 1, 1951

15. Adler, Von M., "Stromung in gekrummten Rohren", Zeitschrift fur Angewandte Mathematic und Mechanik, Ingenieurwissenschaftliche Forschungsorbeiten Band 14, Heft 5, pp. 17-275, 1934

16. Barua, S. N., "On Secondary Flow in Stationary Curved Pipes", Quarterly Journal of Mechanics and Applied Mathematics, Vol. XVI, Pt. 1, pp. 61-77, 1963

17. Barua, S. N., "Secondary Flow in a Stationary Curved Pipe", Fluid Motion Subcommittee, Aeronautical Research Council, F.M. 2162, November, 1954 (AD141862)

18. Ito, Hidesato, "Friction Factors for Turbulent Flow in Curved Pipes", Journal of Basic Engineering", pp. 123-134, June, 1959

19. Weske, J. R., "Investigations of the Flow in Curved Ducts at Large Reynolds Numbers", Journal of Applied Mechanics, pp. 344-348, December, 1948

20. Ito, Hidesato, "On the Pressure Loss of Turbulent Flow through Curved Pipes", The Memoirs of the Institute of High Speed Mechanics, Tohoku University, Vol. 7, pp. 63-76, 1952

BIBLIOGRAPHY

1. Gregory, W. B. and E. W. Schoder, "Some Pitot Tube Studies - The Distribution of Velocities and Pressures in Straight and Curved Portions of a Six-Inch Water Pipe", Transactions of the ASME, Vol. 30, pp. 351-372, (1908)

2. Eustice, John, "Flow of Water in Curved Pipes", Proceedings of the Royal Society, (London), Series A, Vol. 84, pp. 107-118 (1910)

3. Wattendorf, Frank L., "A Study of the Effect of Curvature on Fully Developed Turbulent Flow", Proceedings of the Royal Society (London), Series A, Vol. 148, pp. 565-598 (1934)

4. Davis, George Jacob, Jr., "Investigation of Hydraulic Curve Resistance", Bulletin of the University of Wisconsin No. 408, pp. 115-174, (January, 1910)

5. Keulegan, Garbis H. and K. Hilding Beij, "Pressure Losses for Fluid Flow in Curved Pipes", U.S. Dept. of Commerce, National Bureau of Standards, Research Paper RP 965, Journal of Research of the National Bureau of Standards, Vol. 18, pp. 39-114 (January, 1937)

6. Madison, R. D. and J. R. Parker, "Pressure Losses in Rectangular Elbows", Transactions of the ASME, AER-58-2

7. Kubair, Venugopal and N. R. Kuloor, "Secondary Flow in Helical Coils", Indian Journal of Technology, Vol. 1, pp. 333-335 (September, 1963)

8. Brown, O. G. and A. W. Morris, "Turbulent Flow of Water in Plane Curved Channels of Finite Depth", Journal of Basic Engineering, pp. 377-391 (September, 1963)

9. Marris, A. W., "Radial Distributions of Temporal-Mean Peripheral Velocity and Pressure for Fully Developed Turbulent Flow in Curved Channels", Transactions of the ASME, pp. 528-538 (September, 1960)

10. Eskinazi, Salamon and Hsuan Yeh, "An Investigation on Fully Developed Turbulent Flows in a Curved Channel", Journal of the Aeronautical Sciences, pp. 23-34, 75 (January, 1956)

11. Fox, R. W. and S. J. Kline, "Flow Regimes in Curved Subsonic Diffusers", Journal of Basic Engineering, pp. 303-316 (September, 1962)

12. Squire, H. B. and K. G. Winter, "The Secondary Flow in a Cascade of Airfoils in a Nonuniform Stream", Journal of the Aeronautical Sciences, pp. 271-277 (April, 1951)

13. Vazsonyi, Andrew, "Pressure Losses in Elbows and Duct Branches", Transactions of the A.S.M.E., pp. 177-183 (April, 1944)

14. Locklin, David W., "Energy Losses in 90-Degree Duct Elbows", Heating, Piping and Air Conditioning, pp. 138-145 (September, 1950)

15. Yeh, Hsuan, William G. Rose, Hwachii Lien, "Further Investigations on Fully Developed Turbulent Flows in a Curved Channel", The Johns-Hopkins University Mechanical Engineering Department, Contract Nonr-248(33)-FR, September, 1956 (AD121917)

16. Smith, A. J., "The Flow and Pressure Losses in Smooth Pipe Bends of Constant Cross Section", Journal of the Royal Aeronautical Society, Vol. 67, pp. 437-447, July, 1963

17. Ito, H., "Pressure Losses in Smooth Pipe Bends", Journal of Basic Engineering, pp. 131-143, March, 1960

18. Dimmock, N. A., "Cascade Corners for Ducts of Circular Cross Section", British Chemical Engineering, Vol. 2, No. 6, pp. 302-307, June, 1957

19. Anderson, Alvin G. and Lorenz G. Straub, "Hydraulics of Conduit Bends", St. Antony Falls Hydraulic Laboratory, University of Minnesota, Bulletin No. 1, 1948

20. Straub, Lorenz G. and Edward Silberman, "The Nature of Flow in an Elbow", St. Antony Falls Hydraulic Laboratory, University of Minnesota, Project Report No. 5, 1947 (AT1210545)

21. Richter, Hugo, "Der Druckabfall in gekrummten glatten Rohrleitungen", Forschungsarbeiten auf dem Gebiete des Ingenieurwesens, herausgegeben vom Verein Deutscher Ingenieure, Heft 338, 1930

22. Nippert, H., "Uber den Stromungsverlust in gekrummten Kanalen", Forschungsarbeiten, Auf dem Gebiete des Ingenieurwesens, herausgegeben vom Verein Deutscher Ingenieure, Heft 320, 1929

23. Rouse, Hunter, ed, "Engineering Hydraulics", John Wiley and Sons, Inc., New York (1950)

24. Davies, Powys, and Shivram Vasudeo Puranik, "The Flow of Water through Rectangular Pipe-Bends", Journal of the Institute of Civil Engineers", Vol. 2, pp. 83-135, 1935-36

25. Eastwood, Wilfred, "The Effect of a Transition Curve on the Loss of Head at a Bend in a Pipeline", Proceedings of the Institute of Civil Engineers, pp. 129-143, June, 1960

26. "A Bibliography on the Flow Characteristics of Noncircular Pipes, Ducts and Fittings", The British Hydromechanics Research Association, Bib 6, August, 1962 (N63-20051)

27. "Some Literature References on Pressure Losses in Bends, Diffusers and Bend Diffuser Combinations", The British Hydromechanics Research Association, Bib 7, September, 1962 (N63-20052)

28. Goldstein, S., "Modern Developments in Fluid Dynamics", Oxford Press, Vol. 1, 1938

29. Patterson, G. N., "Corner Losses in Ducts", Aircraft Engineering, pp. 205-208, August, 1937

30. Harper, John J., "Test on Elbows of a Special Design", Journal of the Aeronautical Sciences, pp. 587-592, November, 1946

31. Lansford, Wallace M., "The Use of an Elbow in a Pipe Line for Determining the Rate of Flow in the Pipe", University of Illinois, Bulletin No. 289, December 22, 1936

32. Weske, John R., "Pressure Loss in Ducts with Compound Elbows", National Advisory Committee for Aeronautics, WR-W-39, ARR February, 1943

33. Higginbotham, James T. and Charles C. Wood, "A Study of the High-Speed Performance Characteristics of 90° Bends in Circular Ducts", National Advisory Committee for Aeronautics, Tech. Note 3696, June, 1956 (N62-55696)

34. Wilbur, Stafford W., "An Investigation of Flow in Circular and Annular 90° Bends with a Transition in Cross Section", National Advisory Committee for Aeronautics, Tech. Note 3995, August, 1957 (N62-55995)

35. Hansen, Arthur G., Howard Z. Herzig, and George R. Costello, "Smoke Studies of Secondary Flows in Bends, Tandem Cascades, and High-Turning Configurations", National Advisory Committee for Aeronautics, R.M. E52L24a, March 11, 1953

36. Tones, J R., "Flow of a Non-Newtionian Liquid in a Curved Pipe", Quarterly Journal of Mechanics and Applied Mathematics, Vol. 13, Pt. 4, pp. 429-443, 1960

37. Squire, H. B., "Note on the Secondary Flow in a Curved Circular Pipe", Fluid Motion Subcommittee, Aeronautical Research Council, FM2034, February, 1954 (AD46061) (CONFIDENTIAL)

38. Thom, A. S., "Design of a Right-Angled Bend with Constant Velocities at the Walls", Fluid Motion Subcommittee, Aeronautical Research Council FM1674, February, 1952 (AD4900) (CONFIDENTIAL)

39. Marris, A. W., "The Generation of Secondary Vorticity in an Incompressible Fluid", Journal of Applied Mechanics, pp. 525-531, December, 1963

40. Marris, A. W., "On Fully Developed Turbulent Flow in Curved Channels", Canadian Journal of Physics, Vol. 34, pp. 1134-1146, 1956

41. Marris, A. W., "On the Generation of Secondary Velocity Along a Vortex Line", ASME Paper Number 64-FE-13, 1964

42. Marris, A. W., "Generation of Secondary Vorticity in a Stratified Fluid", March, 1964 (To be published)

43. Marris, A. W., "On the Bending of Streamlines towards Vortex Lines", (To be published)

44. Senoo, Yasutoshi, "Three-Dimensional Laminar Boundary Layer in Curved Channels with Acceleration", Gas Turbine Laboratory, Massachusetts Institute of Technology, Report No. 37, November, 1956

45. Miyagi, Otogoro, "Flow in a Curved Pipe and its Stability", Journal of the Japan Society of Mechanical Engineers, Vol. 35, pp. 1121-1124, 1932 (In Japanese)

46. Kito, Fumiki, "On Secondary Vortex Generated in a Bent-pipe of Elliptical Cross Section", Journal of the Japan Society of Applied Mechanics, Vol. 3, pp. 73-75, 1950 (In Japanese)

47. Tomita, "On the Flow of Water in Coiled Pipes", Journal of the Japan Society of Mechanical Engineers, Vol. 35, pp. 293-304, 1932 (In Japanese)

48. Horlock, J. H., "Some Experiments on the Secondary Flow in Pipe Bends", Proceedings of the Royal Society, Vol. 234, pp. 335-346, February, 1956

49. Hayes, Wallace D., "The Three-Dimensional Boundary Layer", Navord Report 1313, NOTS384, May, 1951

50. Moore, Franklin K., "Three-Dimensional Compressible Laminar Boundary-Layer Flow", National Advisory Committee for Aeronautics, TN 2279

51. Cooke, J. C., "Three-Dimensional Turbulent Boundary Layers", Aeronautical Research Council C.P. No. 635

52. Tetervin, Neal, "Boundary-Layer Momentum Equations for Three-Dimensional Flow", National Advisory Committee for Aeronautics, TN1479, October, 1947

53. Cooke, J. C. and M. G. Hall, "Boundary Layers in Three Dimensions", Advisory Group for Aeronautical Research and Development, AGARD Report 273, April, 1960, and in "Progress in the Aeronautical Sciences", Pergamon Press, Vol. 2, pp. 221-282 (1962)

54. Cooke, J. C., "Approximate Calculation of Three-Dimensional Laminar Boundary Layers", Aeronautical Research Council, R & M No. 3201, 1961

55. Johnston, J. P., "On the Three-Dimensional Turbulent Boundary Layer Generated by Secondary Flow", Journal of Basic Engineering, pp. 233-249, March, 1960

56. Howarth, L., "The Boundary Layer in Three-Dimensional Flow - Part I. Derivation of the Equations for Flow Along a General Curved Surface", Philosophical Magazine, Series 7, Vol. 42, pp. 239-243, 1951

57. Cooke, J. C., "An Axially Symmetric Analogue for General Three-Dimensional Boundary Layers", Aeronautical Research Council, R & M 3200, June, 1959

58. Der, J. and G. S. Raetz, "Solution of General Three-Dimensional Laminar Boundary-Layer Problems by an Exact Numerical Method", Institute of Aeronautical Sciences, Paper No. 62-70, January, 1962

59. Raetz, G. S., "A Method of Calculating Three-Dimensional Laminar Boundary Layers of Steady Compressible Flows", Northrop Aircraft, Inc., NAI-58-73, December, 1957

60. Epstein, Melvin, "A Technique for Solving the Laminar Boundary Layer Equations Applicable to Three-Dimensional Compressible Flows", International Heat Transfer Conference 1961 and 1962, Proceedings of the ASME, pp. 382-390, 1963

61. Birkhoff, Garrett and E. H. Zarantonello, "Jet Wakes and Cavities", Academic Press, Inc., New York, 1957

62. Wislicenus, G. F., "Critical Considerations on Cavitation Limits of Centrifugal and Axial-Flow Pumps", Transactions of the ASME, pp. 1707-1714, November, 1956

63. Wislicenus, G. F., R. M. Watson, and I. J. Karassik, "Cavitation Characteristics of Centrifugal Pumps Described by Similarity Considerations", Transactions of the ASME, pp. 17-24, January, 1939

64. Holl, J. William and George F. Wislicenus, "Scale Effects on Cavitation", Journal of Basic Engineering, pp. 385-398, September, 1961

65. Robertson, J. M., "Tunnels for Hydraulic Investigations", Transactions of the ASME, pp. 95-104, January, 1956

66. Knapp, R. T. and A. Hollander, "Laboratory Investigations of the Mechanism of Cavitation", Transactions of the ASME, pp. 419-435, July, 1948

67. Robertson, J. M., J. H. McGinley, and J. W. Holl, "On Several Laws of Cavitation Scaling", LaHouille Blanche, No. 4, pp. 550-554, September, 1957

68. Sarosdy, L. R. and A. J. Acosta, "Note on Observations of Cavitation in Different Fluids", Journal of Basic Engineering, pp. 399-400, September, 1961

69. Jacobs, R. B. and K. B. Martin, "Cavitation Problems in Cryogenics", Transactions of the ASME, pp. 756-757, September, 1960

70. Holl, J. W., "An Effect of Air Content on the Occurrence of Cavitation", Journal of Basic Engineering, pp. 941-946, December, 1960

71. Wang, P. K. C. and J. T. S. Ma, "Cavitation in Valve-Controlled Hydraulic Actuators", Journal of Applied Mechanics, pp. 537-546, December, 1963

72. Holl, J. W., "The Inception of Cavitation on Isolated Surface Irregularities", Journal of Basic Engineering, pp. 169-183, March, 1960

73. Danel, Pierre and Jacques Duport, "The Selection of Length and Head Scales for Cavitation Tests", Transactions of the ASME, pp. 784-794, December, 1960

74. Plesset, M. S., "The Dynamics of Cavitation Bubbles", Journal of Applied Mechanics", pp. 277-282, September, 1949

75. Kermeen, R. W., J. T. McGraw, and B. R. Parkin, "Mechanism of Cavitation Inception and the Related Scale-Effects Problem", Transactions of the ASME, pp. 539-552, October, 1945

76. Stepanoff, A. J., "Cavitation in Centrifugal Pumps", Transactions of the ASME, pp. 533-541, May, 1955

77. Wu, T. Yag-Tsu, "A Free Streamline Theory for Two-Dimensional Fully Cavitated Hydrofoils", Journal of Mathematics and Physics, Vol. 35, pp. 236-265, 1957

78. Watson, R. M., "Cavitation in Centrifugal Pumps - Some of the Less Well-Known Factors", Proceedings of the National Conference on Industrial Hydraulics, Chicago, pp. 50-65

79. McCormick, R. W., Jr., "On Cavitation Produced by a Vortex Trailing from a Lifting Surface", Journal of Basic Engineering, pp. 369, September, 1962

80. Stripling, L. B. and A. J. Acosta, "Cavitation in Turbopumps - Part 1", Transactions of the ASME, pp. 326-338, September, 1962

81. Stripling, L. B. and A. J. Acosta, "Cavitation in Turbopumps - Part 2", Journal of Basic Engineering, pp. 339-350, September, 1962

82. Salemann, Victor, "Cavitation and NPSH Requirements of Various Liquids", Journal of Basic Engineering, pp. 167-173, June, 1959

83. Ruggeri, Robert S. and Thomas F. Gelder, "Effects of Air Content and Water Purity on Liquid Tension at Incipient Cavitation in Venturi Flow", National Aeronautics and Space Administration, TN D-1459, March, 1963

84. Ruggeri, Robert S. and Thomas F. Gelder, "Cavitation and Effective Liquid Tension of Nitrogen in a Tunnel Venturi", National Aeronautics and Space Administration, TN D-2088, February, 1964

85. Lewis, George W., Edward R. Tysl, "Cavitation Performance of an 83° Helical Inducer Operated in Liquid Hydrogen", National Aeronautics and Space Administration, TM X-419, March, 1961 (CONFIDENTIAL)

86. Thomas, Harold A. and Emil P. Schuleen, "Cavitation in Conduits", Transactions of the ASCE, Vol. 107, p. 421, 1942

87. Song, C. S. and F. Y. Tsai, "Unsteady, Symmetrical, Supercavitaling Flows Past a Thin Wedge in a Solid Wall Channel", St. Antony Falls Hydraulic Laboratory, University of Minnesota, Tech. Paper No. 38, Series B, June, 1962

88. Wu, T. Yao-tsu and D. P. Wang, "An Approximate Numericial Scheme for the Theory of Cavity Flows Past Obstacles of Arbitrary Profile", Hydrodynamics Laboratory, California Institute of Technology, Report No. 111-1, July, 1963

89. Wu, T. Yao-tsu and D. P. Wang, "A Wake Model for Free-Streamline Flow Theory, Part II. Cavity Flows Past Obstacles of Arbitrary Profile", Hydrodynamics Laboratory, California Institute of Technology, Report No. 97-4, May, 1963

90. "Cryogenic Fluid Cavitation Study Final Report Static Phase", National Bureau of Standards, Technical Documentary Report No. RTD-TDR-63-1035

91. Treaster, Allen L., "Cavitation Hysteresis", M.S. Thesis, Pennsylvania State University, June, 1964 (AD-436602)

92. Dryden, Hugh L., Francis D. Murraghan and H. Bateman, "Hydrodynamics", Dover Publications, 1956